DEEP-SEA RESEARCH
PART I

Biogeochemical flux and phytoplankton succession: A year-long sediment trap record in the Australian sector of the Subantarctic Zone

CrossMark

Jessica V. Wilks[a,*], Andrés S. Rigual-Hernández[a,b], Thomas W. Trull[c,d], Stephen G. Bray[c], José-Abel Flores[b], Leanne K. Armand[a]

[a] MQ Marine Research Centre and Department of Biological Sciences, Macquarie University, North Ryde, NSW 2109, Australia
[b] Department of Geology. Universidad de Salamanca, Salamanca 37008, Spain
[c] Antarctic Climate and Ecosystems Cooperative Research Centre, University of Tasmania, Hobart, Tasmania 7001, Australia
[d] CSIRO Oceans and Atmosphere Flagship, Hobart, Tasmania 7001, Australia

ABSTRACT

The Subantarctic Zone (SAZ) plays a crucial role in global carbon cycling as a significant sink for atmospheric CO_2. In the Australian sector, the SAZ exports large quantities of organic carbon from the surface ocean, despite lower algal biomass accumulation in surface waters than other Southern Ocean sectors. We present the first analysis of diatom and coccolithophore assemblages and seasonality, as well as the first annual quantification of bulk organic components of captured material at the base of the mixed layer (500 m depth) in the SAZ. Sediment traps were moored in the SAZ southwest of Tasmania as part of the long-term SAZ Project for one year (September 2003 to September 2004). Annual mass flux at 500 m and 2000 m was composed mainly of calcium carbonate, while biogenic silica made up on average < 10% of material captured in the traps. Organic carbon flux was estimated at $1.1 \text{ g m}^{-2} \text{ y}^{-1}$ at 500 m, close to the estimated global mean carbon flux. Low diatom fluxes and high fluxes of coccoliths were consistent with low biogenic silica and high calcium carbonate fluxes, respectively. Diatoms and coccoliths were identified to species level. Diatom and coccolithophore sinking assemblages reflected some seasonal ecological succession. A theoretical scheme of diatom succession in live assemblages is compared to successional patterns presented in sediment traps. This study provides a unique, direct measurement of the biogeochemical fluxes and their main biological carbon vectors just below the winter mixed layer depth at which effective sequestration of carbon occurs. Comparison of these results with previous sediment trap deployments at the same site at deeper depths (i.e. 1000, 2000 and 3800 m) documents the changes particle fluxes experience in the lower "twilight zone" where biological processes and remineralisation of carbon reduce the efficiency of carbon sequestration.

1. Introduction

The Subantarctic Zone (SAZ) is the northernmost zone of the Southern Ocean, delineated by the Subtropical Front to the north and the Subantarctic Front to the south. The SAZ is the Southern Ocean's warmest zone, and comprises > 50% of its surface area (Orsi et al., 1995). Yet, the SAZ is a High-Nitrate, Low-Chlorophyll (HNLC) zone due to low phytoplankton biomass production, despite the excess in nitrate and phosphate in surface waters (Bucciarelli et al., 2001). Strong silicate and iron limitation (Blain et al., 2001; Hutchins et al., 2001; Fripiat et al., 2011), as well as light limitation due to deep winter mixing, each contribute to the zone's HNLC status (Bucciarelli et al., 2001; Trull et al., 2001c). Nonetheless, the SAZ is significant as one of the strongest oceanic sinks of atmospheric CO_2 in global climate (Metzl

et al., 1999; Trull et al., 2001c; Shadwick et al., 2015), driven by phytoplankton primary production and subsequent particle export (i.e. the biological pump), and by uptake via dissolution in newly formed waters (i.e. the solubility pump) (Honjo et al., 2000; Trull et al., 2001c).

Sediment traps measure biological and particulate matter exported from the photic zone to the ocean interior, providing insights into oceanic particle flux and phytoplankton ecology (e.g. Honjo et al., 2008; Romero and Armand, 2010). The multidisciplinary SAZ Project was initiated in 1997 by the Antarctic Cooperative Research Centre (ACE CRC) in Tasmania to remedy the lack of oceanographic data within the SAZ and the Polar Frontal Zone (PFZ) (Trull et al., 2001c). The SAZ Project deployed bottom-tethered sediment traps to quantify and characterise the particle fluxes from the Subantarctic to the Antarctic along 140°E, enabling comparisons between zones (Trull
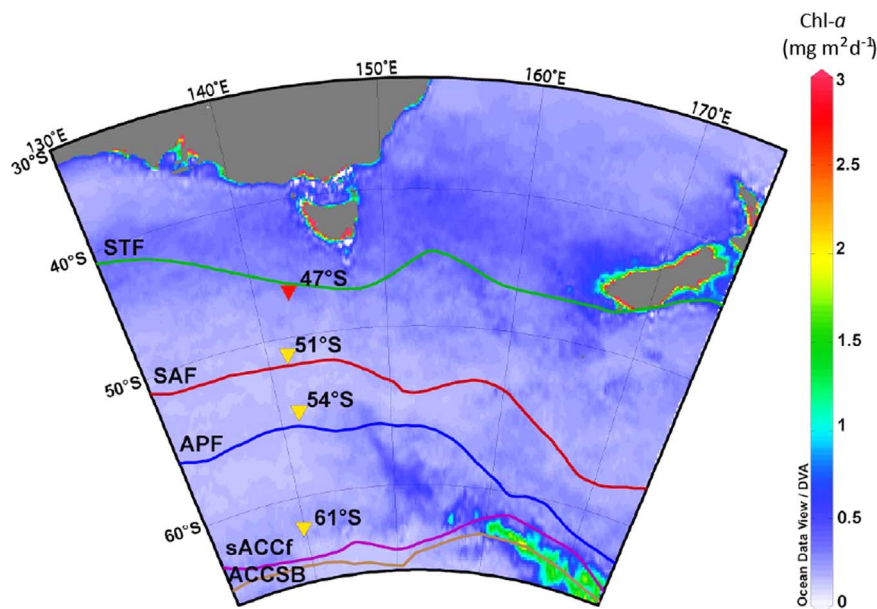
Fig. 1. Regional context of sediment trap deployment (SAZ Project) 2003–2004 showing fronts and zones (adapted from Orsi et al., 1995). Triangles indicate SAZ Project sediment trap deployment locations; red triangle shows current site at 47°S. Lines indicate front locations, from top to bottom: Subtropical Front (STF) green line; Subantarctic Front (SAF) red line; Antarctic Polar Front (APF) blue line; south Antarctic Circumpolar Current front (sACCf) purple line; Antarctic Circumpolar Current Southern Boundary (ACCSB) brown line. Coloured bar denotes Chlorophyll-a concentrations (mg m^2 d^{-1}), August 2003 to August 2004. Map created with Ocean Data View, available at http://odv.awi.de (Schlitzer, 2016).

et al., 2001c, 2001a; Rigual-Hernández et al., 2015a, 2016b). The SAZ Project also allowed comparison to other particle flux studies in nearby regions, such as the Antarctic Environment and Southern Ocean Process Study (AESOPS), which deployed sediment traps in the SAZ, PFZ, AZ, and Ross Sea along 170°W (Smith et al., 2000; Honjo et al., 2000; Anderson and Smith, 2001), the Subantarctic National Institute of Water and Atmospheric Research (NIWA) studies (Nodder and Northcote, 2001); and trapping studies in the Atlantic sector (Wefer and Fischer 1991; Fischer et al., 2002). Early results of the SAZ Project time-series traps focused on the bulk particulate components, reporting lower algal biomass accumulation in the Australian sector than in the Atlantic or New Zealand sectors of the SAZ (Rintoul and Trull, 2001; Trull et al., 2001a), although total particulate organic carbon flux was similar to the global ocean median (Lampitt and Antia, 1997).

A series of papers succeeding the SAZ Project have contributed to our understanding of production and carbon fluxes in the Australian sector across oceanographic zones, and the influence of phytoplankton assemblages on Southern Ocean biogeochemistry (Ebersbach et al., 2011; De Salas et al., 2011; Rigual-Hernández et al., 2015a, 2015b). Work remains to be undertaken to quantify the carbon exporting capacity of the range of phytoplankton species in this region.

Diatoms are a diverse group of unicellular phytoplankton that occur in high abundances in the Southern Ocean (Alvain et al., 2008), and are the most significant contributors of biogenic silica to the Southern Ocean's sediments, particularly south of the Polar Front (Ragueneau et al., 2000; Rigual-Hernández et al., 2016). Both live and sediment-trap records of diatom assemblages have been studied in the Australian sector (De Salas et al., 2011; Kopczyńska et al., 2007; Rigual-Hernández et al., 2015a; Rigual-Hernández et al., 2015b). Analyses of live coccolithophore assemblages (Nishida, 1986; Findlay and Giraudeau, 2000), and past and present calcification (Cubillos et al., 2007, 2012), have also been conducted in the Australian sector whilst seafloor sediment core-top analyses have recently revealed that coccoliths comprise a significant percentage of sediment in the Pacific sector of the SAZ (Saavedra-Pellitero et al., 2014). Sediment traps deployed near the Crozet Plateau (PFZ) revealed that coccoliths were responsible for roughly a third of particulate inorganic carbon (PIC) export (Salter et al., 2014), while coccoliths made up > 85% PIC exported over the Kerguelen Plateau (AZ) (Rembauville et al., 2016). Yet despite their

significance to PIC production and export, coccolithophore fluxes have not been quantified within the pelagic waters of the SAZ.

To address the need for a comprehensive understanding of the major biological export flux taxa and their seasonal contribution to particle export in the Australian sector of the SAZ, this study returns to the SAZ Project trap programme's 47°S trap sample splits (Sept. 2003–Oct. 2004, 47°S, 140°E; 500 m and 2000 m depth). This new investigation on the preserved material enables:

1) A description of temporal seasonality and composition of particle fluxes at the base of the mixed layer in the SAZ, and
2) The documentation of assemblage composition of two of the main groups of phytoplankton in the region: diatoms and coccolithophores.

Aim 1 delivers the first annual quantification of biogenic silica, calcium carbonate and POC export for the Australian sector of the SAZ at the base of the winter mixed layer. The second aim provides the first report of seasonal variability of diatom and coccolithophore assemblages for the pelagic waters of the SAZ in the Southern Ocean. Additionally, we present a comparison of how theoretical live diatom ecological succession is reflected in sediment trap records.

1.1. Oceanographic setting

The Southern Ocean is banded by approximately concentric zones of water masses (Orsi et al., 1995), possessing distinct and relatively uniform hydrological properties that influence the phytoplankton species found (Boyd et al., 2000; Sokolov and Rintoul, 2002; Pollard et al., 2002) (Fig. 1). These water masses make up the Antarctic Circumpolar Current (ACC), which includes, from north to south, the Subantarctic Zone (SAZ), Polar Frontal Zone (PFZ), and the Antarctic Zone (AZ). Zones are defined by the fronts at which they meet, where the characteristics of the water masses (particularly temperature and salinity) sharply change. The SAZ stretches from the Subtropical Front (STF), the boundary between subtropical and subantarctic waters to the north (44.5–45.6°S in the Australian region), to the Subantarctic Front (SAF), the strongest front within the ACC (50–53°S) (Sokolov and Rintoul, 2002). The water masses of the SAZ are stratified in

austral summer, with stratification controlled mainly by temperature, and weakening stratification in winter (Rintoul and Trull, 2001; Pollard et al., 2002). In this study, we use the front definitions of Orsi et al. (1995).

The trap deployment site (46°48′S, 142°6′E) is biogeochemically typical of the SAZ, being low in silica and iron year-round but replete in nitrate (Rintoul and Trull, 2001; Sedwick et al., 1999, 2008). The site is representative of the SAZ between 90° and 145°E (Trull et al., 2001a). The SAZ has a deep mixed layer in winter (up to 600 m during more extreme years) that shallows to 75–100 m in summer (Rintoul and Trull, 2001; Trull et al., 2001c). In general, the mixed layer is deeper than the euphotic zone in this region throughout the year. The euphotic zone (the depth at which PAR is 1% of the surface incident PAR) ranges from ~115 m in winter, when phytoplankton abundance is lowest, to ~45 m in summer when algal biomass reaches maximal values (Westwood et al., 2011). During sunny, calm weather in summer, the mixed layer can be shallower (to ~25 m) than the euphotic zone, and production below the mixed layer may reach 10% of the total water column production (Westwood et al., 2011). These conditions are short-lived and chlorophyll fluorescence profiles show that phytoplankton biomass is distributed uniformly within the mixed layer without subsurface maxima (Rintoul and Griffiths, 2001; Bowie et al., 2011). Regionally, the SAZ has slightly higher silicate and slightly deeper mixed layer depths to the south due to the input of cooler, fresher water moving northwards across the SAF. Such differences in hydrological properties between the north and south of the SAZ are more pronounced during summer than winter (Lourey and Trull, 2001; Rintoul and Trull, 2001).

2. Materials and methods

2.1. Field Experiment

McLane PARFLUX sediment traps (0.5 m^2 capture area) were deployed for one year (2003–2004) in the Australian sector of the Subantarctic Zone (46°46′ S, 142°4′ E) via the SAZ Project (Trull et al., 2001c) (Fig. 1). Traps were deployed on one mooring line at 500 m, 1000 m and 2000 m, however, the 1000 m trap captured little material and was not analysed.

The 500 m trap was equipped with a tilt meter, and an Aanderaa RCM8 current meter placed 50 m below it on the mooring line. Current speeds for the duration of the deployment averaged 10.9 cm s^{-1} (Supplementary Table 1); slightly below speeds at which trapping efficiency is considered to decrease (~12 cm s^{-1}; Baker et al., 1988). There were occasional short excursions to higher velocities during the autumn and winter months, however, 95% of the time current speeds were below 23 cm s^{-1}.

Each trap consisted of 21×500 mL collection cups rotated on a 14 d (summer and spring) or a 35 d (autumn and winter) pre-programmed schedule. All traps successfully completed collection for the entire sampling period, though some cups contained too little material to analyse. At 500 m, cup 12 was omitted from analyses, while for the 2000 m trap, only cups 1 − 11 (spring to summer) and 17 (autumn) were exploitable for this study as the remaining cups captured too little material to analyse (Supplementary Table 1). Sampling dates and lengths are given in Table 1.

After retrieval, samples were sieved with a 1 mm sieve to remove large swimmers. Samples were split into ten fractions using a McLane rotary splitter, and were stored at 4 °C in the dark in 50 mL tubes (Bray et al., 2000; Trull et al., 2001b).

2.2. Biogeochemical flux determination

Detailed explanation of Total Mass Flux (TMF), Particulate Organic Carbon (POC), calcium carbonate (CaCO$_3$), and Biogenic Silica (BSi) calculations are given in Bray et al. (2000) and Trull et al. (2001a).

POC, CaCO$_3$ and BSi were not calculated for cups 13–21 at 2000 m, as too little material was captured. Annual TMF was calculated for the 500 m trap only, as the 2000 m trap did not contain an entire year's useable samples. Three 1/10 splits of the < 1 mm fraction were stored for later microscopic analyses. The remainder was filtered, dried, weighed, and ground. Samples were filtered using 0.4 μm Millipore polycarbonate membranes. Samples were dried at 60 °C in a forced convection oven. Particulate inorganic carbonate (PIC) was measured by adding phosphoric acid to the dry sample, and measuring CO$_2$ produced using a colourimeter. Total particulate carbon (PC) and nitrogen (PN) were determined using a Perkin Elmer CHN Analyser, and POC was estimated by difference, i.e. POC=PC−PIC. BSi was estimated using hot alkaline digestion and visible spectrometry following Quéguiner (2001).

2.3. Siliceous microplankton preparation and identification

One 1/10 split of the sieved fraction was used for the biological flux analyses. This split was topped up to 40 mL using distilled water, and a 10 mL subsample was taken for coccolith analyses. The remaining split was cleaned of organic material using potassium permanganate, hydrochloric acid, and hydrogen peroxide as per Romero et al. (1999). After organic material removal, samples were centrifuged, the supernatant removed, and topped up with distilled water.

Slides were prepared using a modified form of the random settling method (Flores and Sierro, 1997), to ensure even diatom distribution within the suspension to avoid frustule overlap or clumping on slides. A known fraction (4 mL standard, up to 25 mL for very sparse samples) of the diatom suspension was used to make three microscope slides/ sample.

The slides were analysed using an Olympus BH-2 compound light microscope at 1000x magnification. Counts were undertaken along non-overlapping transects on each slide, evenly spaced and avoiding coverslip edges. All diatoms within the field of view along each transect were visually identified to species or genus level and 400 individual diatoms were counted per sample (Armand and Leventer, 2010). Winter cup sample splits contained sparse material, so for these samples, the enumeration protocol was lowered to 100 individuals (Fatela and Taborda, 2002). Samples containing fewer than 100 diatoms are indicated with asterisks in Supplementary Tables 2a and 2b.

Taxonomic identification followed modern taxonomy as per Hasle and Syvertsen (1997). Diatoms that could not be identified to genus level were placed into additional categories: unknown pennate, unknown centric, and unknown centric < 20 μm. One group of diatoms could not be identified past genus level and was named "Thalassiosira sp. 1" (Rigual-Hernández et al., 2015b). This grouping contained centric diatoms larger than 20 μm with radial-style areolation, appearing to be poorly-preserved valves of the genus Thalassiosira. The resting spores of Chaetoceros species were grouped simply as Chaetoceros resting spores.

2.4. Calcareous microplankton sample preparation and identification

A 10 mL subsample of each split was removed prior to acid digestion to allow an analysis of the coccolithophore community assemblage and flux. The entire 10 mL subsample was used to prepare slides for light microscopy. As flux captured in the traps was low, due to limited material SEM analysis of coccoliths was not undertaken. Slides were prepared as per diatoms. Coccoliths were counted under 1000× magnification using a LEICA DMRXE polarised light microscope, and 300 coccoliths were identified per sample.

Identification of coccolithophore taxa followed Young et al. (2003) and Young et al. (2014). In total eleven coccolithophore taxa were identified from coccoliths. Only few coccospheres were detected in the samples, most likely due to the fact that the majority of the material

Table 1

Daily and annual fluxes of total mass flux, biogenic silica (BSiO2), calcium carbonate (CaCO3), particulate organic carbon (POC), diatom and coccolith flux, and Shannon's Equitability Index (Eh), for every cup at both trap depths (500 m and 2000 m). * indicates "annualised values." Mean annual bulk component fluxes were not calculated for the 2000 m trap due to lack of cups retrieved. Mean flux spring/summer† refers to the overlapping sampling period (spring and summer; cups 1–11) in which enough material was captured for analysis at both 500 m and 2000 m traps.

Cup #	Sampling midpoint	Sampling length (days)	Total Mass Flux (mg m^{-2} d^{-1})	BSiO$_2$ (mg m^{-2} d^{-1})	(%)	CaCO$_3$ (mg m^{-2} d^{-1})	(%)	POC (mg m^{-2} d^{-1})	(%)	Diatom flux (x10^3 valves m^{-2} d^{-1})	Coccolith flux (x10^6 coccoliths m^{-2} d^{-1})	Shannon's Equitability Eh
500 m												
1	28/09/2003	14	26.2	1.88	7.2	16.5	63	2.7	10.2	28.3	310	0.70
2	12/10/2003	14	106.8	7.66	7.2	80.1	75	6.8	6.4	721.3	720	0.75
3	26/10/2003	14	59.3	3.06	5.2	44.4	75	4.4	7.4	229.7	825	0.72
4	9/11/2003	14	123.3	7.86	6.4	100.8	82	6.5	5.3	1248.6	1539	0.76
5	23/11/2003	14	139.1	8.79	6.3	105.1	76	8.9	6.4	810.2	2543	0.70
6	7/12/2003	14	174.6	13.59	7.8	132.0	76	11.1	6.3	7384.3	5203	0.69
7	21/12/2003	14	16.6	0.83	5.0	11.4	69	1.7	9.9	13.6	482	0.67
8	4/01/2004	14	9.0	0.37	4.1	6.5	72	0.8	9.1	12.7	205	0.67
9	18/01/2004	14	3.5	0.14	4.1	2.4	69	0.4	10.8	0.8	79	0.82
10	1/02/2004	14	6.1	0.25	4.1	4.2	69	0.7	10.8	1.5	81	0.70
11	15/02/2004	14	0.7	0.03	4.1	0.5	69	0.1	10.8	0.2	13	0.95
13	14/03/2004	14	16.9	0.54	3.2	11.1	65	2.1	12.5	64.6	221	0.63
14	28/03/2004	14	1.6	0.06	3.8	1.2	71	0.2	9.4	0.2	27	0.93
15	11/04/2004	14	2.8	0.11	3.8	2.0	71	0.3	9.4	0.4	58	0.58
16	25/04/2004	14	1.3	0.05	3.8	0.9	71	0.1	9.4	0.4	31	0.34
17	19/05/2004	35	0.2	0.01	3.8	0.1	71	0.0	9.4	0.03	5	0.77
18	23/06/2004	35	0.8	0.03	3.8	0.6	71	0.1	9.4	0.2	29	0.65
19	28/07/2004	35	0.3	0.01	3.8	0.2	71	0.0	9.4	0.09	4	0.19
20	1/09/2004	35	1.3	0.05	3.8	0.9	71	0.1	9.4	0.2	48	0.80
21	26/09/2004	14	533.1	23.41	4.4	411.1	77	33.8	6.3	5750.1	23221	0.59
Mean daily flux			**47.2**	**2.6**	**4.78**	**35.9**	**71.73**	**3.1**	**8.91**	**813.38**	**1782.22**	
Mean flux spring/summer†			**60.5**	**4.0**	**6.6**	**45.8**	**75.7**	**4.0**	**6.6**	**950.1**	**1091.0**	
Annual flux (g m^{-2} y^{-1})			17*	0.9		13.1		1.1		2.3 × 10^8 m^{-2} y^{-1}	6.5 × 10^{11} m^{-2} y^{-1}	
Mean Eh												**0.68**
2000 m												
1	28/09/2003	14	23.1	1.9	8.3	18	76	1.38	6.0	36	78	0.78
2	12/10/2003	14	60.9	5.0	8.2	47	77	2.84	4.7	103	340	0.74
3	26/10/2003	14	52.2	4.1	7.8	39	76	2.48	4.8	169	458	0.76
4	9/11/2003	14	52.8	3.4	6.5	42	80	2.24	4.2	95	551	0.73
5	23/11/2003	14	125.0	8.7	6.9	98	78	6.11	4.9	892	1911	0.78
6	7/12/2003	14	152.2	12.3	8.1	119	78	7.36	4.8	1699	2304	0.71
7	21/12/2003	14	138.7	12.9	9.3	110	79	5.29	3.8	1081	3356	0.71
8	4/01/2004	14	74.5	6.4	8.6	58	78	3.00	4.0	326	1454	0.70
9	18/01/2004	14	118.4	14.7	12.4	86	73	5.34	4.5	1258	1316	0.70
10	1/02/2004	14	171.7	16.9	9.9	129	75	8.47	4.9	2724	1201	0.68
11	15/02/2004	14	161.1	21.3	13.2	106	66	10.86	6.7	3650	891	0.68
17	19/05/2004	35								0.39	5.01	0.80
Mean flux spring/summer†			**102.76**	**9.79**	**9.03**	**77.53**	**76.10**	**5.03**	**4.85**	**1093.82**	**1260.09**	
Annual flux (g m^{-2} y^{-1})			38*	–	–	–	–	–	–	–	–	
Mean Eh												**0.73**

sinking out of the mixed layer in this region has been heavily processed by phytoplankton (Ebersbach, 2011). In addition, it is possible that some disaggregation of coccoliths from coccospheres may have occurred during sample storage, splitting and sample processing. It is worth noting that the 47°S sediment trap site location is considered representative of a large portion of the zonal SAZ (i.e. between 90 and 145°E; Trull et al., 2001c). Therefore, even if some coccoliths would have been laterally transported from a relatively distant area, it is likely that the sinking coccolith assemblages captured by the traps are still representative of the homogenous environmental conditions this sector of the SAZ. While *Gephyrocapsa muellerae* and *G. oceanica* were counted separately, coccoliths that were clearly of the genus *Gephyrocapsa*, but < 3 µm in diameter, were placed in their own grouping (*Gephyrocapsa* < 3 µm) (Flores et al., 2000). The grouping *Gephyrocapsa* < 3 µm contained *G. ericsonii* and *G. ampliaperta*, both

of which are difficult to discern under light microscopy. Most of the specimens of *Calcidiscus leptoporus* were subspecies *leptoporus*, however some of the small *C. leptoporus* complex were occasionally encountered. Coccoliths attributed to the genera *Syracosphaera, Pontosphaera, Oolithothus* and *Umbilicosphaera* were not identified past genus level.

2.5. Flux calculations and statistics

Raw counts per sample were transformed into daily fluxes using the following equation (Sancetta and Calvert 1988):

$$\text{Valve or coccolith flux } m^{-2}d^{-1} = \left(\frac{N \cdot \left(\frac{A}{a}\right) \cdot \left(\frac{V}{v}\right)}{D \cdot T} \right)$$

where N is the number of specimens counted, A is the area of the petri dish upon which the slide was made, a is the area of the slide counted, V is the volume of the diluted total sample, v is the volume of the split of each cup, D is the number of days of trap deployment, and T is the area of the sediment trap opening in m^2. For the diatom flux calculations, a modifier was applied after flux was calculated to compensate for the 10 mL subsample for the calcareous phytoplankton. For graphing, fluxes were transformed into relative abundances.

The Shannon-Weaver Equitability index (E_h) was used to estimate the diversity and evenness of species assemblages (Shannon and Weaver, 1949). E_h values range between zero and one, with values close to zero indicating poor diversity and evenness, and values close to one indicating high diversity and evenness.

A table of correlation matrices was constructed in order to identify relationships present between diatom and coccolith flux, and annual biogeochemical fluxes.

2.6. Meteorological and environmental data

Photosynthetically Active Radiation (PAR), chlorophyll-*a* concentration (Chl-*a*) and Sea Surface Temperature (SST) data for the trap deployment period (Aug. 2003–Oct. 2004) were obtained from the Goddard Earth Sciences Data and Information Services Centre (GES DISC) for the area 48° 30′ 0″ S–46° 30′ 0″ S×130° 0′ 0″ E–150° 0′ 0″ E (Fig. 2a; Supplementary Table 3).

2.7. Canonical correspondence analysis

Canonical Correspondence Analysis (CCA) was conducted using the free software PAST (Hammer et al., 2001). Fluxes were normalised with a log10 transformation, and CCA was applied to 19 diatom species of greater than 0.5% relative abundance present at 500 m, and to the eight coccolithophore taxa observed in two or more cups at 500 m. The environmental constraints applied were SST and PAR for both groups (Supplementary Table 3). Diatom and coccolithophore taxa groupings that emerged from the CCA were combined by relative abundance, and plotted separately over time.

3. Results

3.1. Satellite-derived environmental parameters

Photosynthetically Active Radiation (PAR) increased gradually from 21 Einstein m^{-2} d^{-1} at the beginning of the time series, and peaked in December at 45.1 Einstein m^{-2} d^{-1} (Fig. 2a; Supplementary Table 3). Then PAR values steadily decreased over autumn, reaching the annual minimum by June. Sea Surface Temperature (SST) increased slowly during spring, beginning to rise nearly 2 months after the winter-to-spring PAR increase, and eventually peaked in late December at 11 °C (Fig. 2a; Supplementary Table 3). Minimum SST was observed in June (8.3 °C). Chlorophyll-*a* concentrations in surface waters ranged from the summer maximum of 0.317 mg m^{-3}, occurring
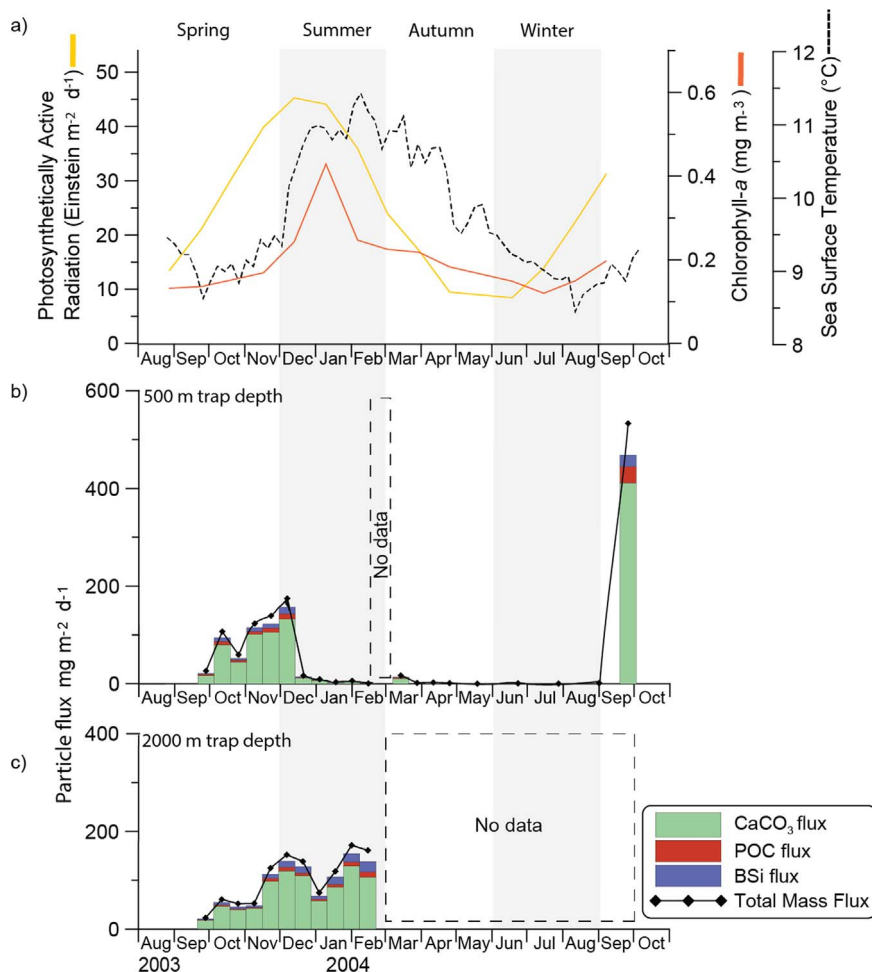

Fig. 2. Surface environmental parameters, and particle flux measurements at 500 m and 2000 m traps across the 2003–2004 study period. (a) Photosynthetically Active Radiation (PAR) (yellow line), Chlorophyll-a concentration (orange line) and Sea-Surface Temperature (SST) (black dotted line), across sampling year; (b) Carbonate (CaCO$_3$) (green bar), Particulate Organic Carbon (POC) (red bar), Biogenic Silica (BSi) (blue bar), and total mass flux (black line) at 500 m trap across sampling year; (c) CaCO$_3$, POC, BSi, and total mass flux at 2000 m trap across sampling year.

in late December, to winter lows of 0.12 mg m^{-3} in July (Fig. 2a; Supplementary Table 3).

3.2. Mean total mass flux and seasonality

Total Mass Flux (TMF) was calculated for the entire sampling period for 500 m (Fig. 2b; Table 1), but was only calculated for spring and summer (September-February) at 2000 m as capture was too low for the rest of the sampling year (see Section 2.1) (Fig. 2c; Table 1). TMF at 500 m ranged from a peak of 175 mg m^{-2} d^{-1} during the summer maximum in December, and dropped to below 3 mg m^{-2} d^{-1} for 6 months of the year (Table 1), and approximately 50% of the TMF accumulated between October and early December (Fig. 2b). An exceptionally high TMF value of 533 mg m^{-2} d^{-1} was recorded in a peak-flux event in September 2004 at 500 m (Fig. 2b; Table 1).

A first peak in TMF at 2000 m (152 mg m^{-2} d^{-1}) was captured in December, coinciding with the TMF peak at 500 m (Fig. 2c; Table 1). A second TMF peak, and the maximum observed at 2000 m at 172 mg m^{-2} d^{-1}, occurred in February (Fig. 2c; Table 1). Mean annual TMF was calculated at 17 g m^{-2} d^{-1} at 500 m, but was not estimated at 2000 m as capture was too low after the spring/summer months (Table 1).

The mean annual contributions of the three major components of biogeochemical flux, CaCO$_3$ POC and BSi, were calculated for the 500 m trap (Table 1). Annual values could not be determined for the 2000 m trap (see above), however mean spring/summer fluxes were calculated. CaCO$_3$ represented the bulk of TMF during the spring/summer period, averaging 76% of TMF at both trap depths (Figs. 2b and 2c; Table 1). CaCO$_3$ flux peaked in early December at 500 m, however, maximum CaCO$_3$ flux occurred during the September 2004 peak-flux event (Fig. 2b; Table 1). At 2000 m, CaCO$_3$ flux peaked in December, and reached a maximum in February (129 mg m^{-2} d^{-1}) (Fig. 2b; Table 1). POC flux during the spring/summer period averaged 7% and 5% of annual TMF at 500 m and 2000 m, respectively (Table 1). POC flux followed a similar trend at both depths, with small flux peaks in December, followed by maxima occurring simultaneously in February (Table 1). BSi fluxes were the most variable of the bulk components at 500 m. BSi made up on average 7% and 9% of TMF at 500 m and 2000 m over the spring/summer period, respectively (Table 1). BSi fluxes, as per the other bulk components, peaked in December, however maximum BSi flux was registered in the September 2004 peak-flux event (Table 1).

3.3. Diatom and coccolith total fluxes

Mean annual diatom and coccolith fluxes at 500 m were 2.3×10^8 valves m^{-2} y^{-1}, and 6.5×10^{11} coccoliths m^{-2} yr^{-1}, respectively (Table 1). Mean annual flux values of diatoms and coccoliths were not determined for the 2000 m trap, as too little material was captured after February (see Section 2.1).

At 500 m, diatom flux increased gradually from September to November, and peaked sharply to reach a maximum of 7.4×10^6 valves m^{-2} d^{-1} in December (Fig. 3a; Table 1). A second maximal peak occurred in the September 2004 peak-flux event (Fig. 3a; Table 1). From mid-summer through winter (January to September) diatom flux was low (a few hundred valves m^{-2} d^{-1}), with the exception of a small peak event in March (Fig. 3a; Table 1).

At the 2000 m trap, diatom flux increased from the beginning of the sample period to peak first in December, and again in February at which time peak fluxes occurred (3.7×10^6) (Fig. 3b; Table 1). Only one cup exists for the period after February at 2000 m (May), in which diatom fluxes were low (3.9×10^2 valves m^{-2} d^{-1}) (Fig. 3b; Table 1).

At 500 m, coccolith fluxes increased gradually between the start of sampling and spring/summer peak fluxes of 5.2×10^9 coccoliths m^{-2} d^{-1} in December (Fig. 3a; Table 1). Coccolith fluxes declined sharply in late December following the peak, and remained low until the
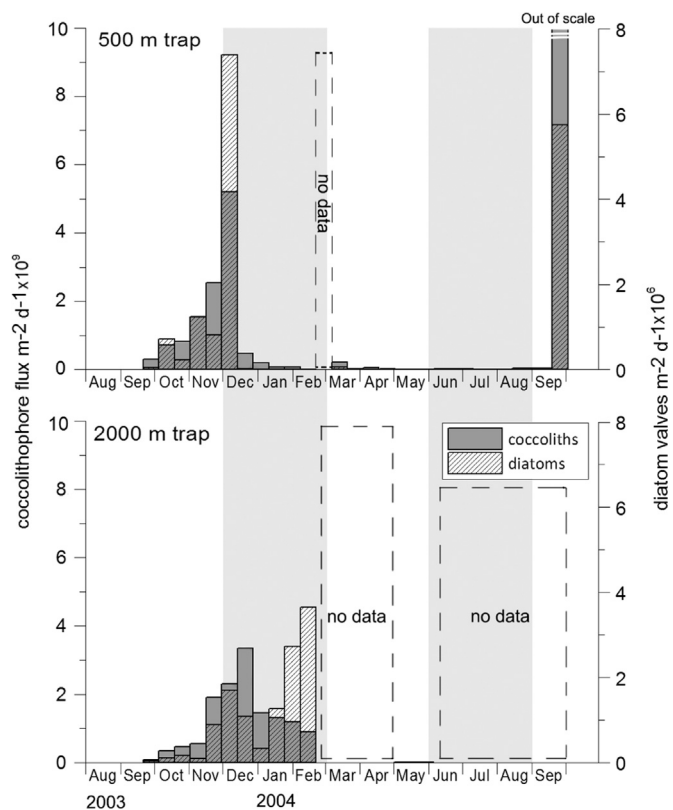

Fig. 3. Coccolith flux (coccoliths m^{-2} d^{-1}, solid grey bars), and diatom flux (valves m^{-2} d^{-1}, hashed bars) at (A) 500 m trap depth, and (B) 2000 m trap depth across the sampling year. Boxes delineated by dotted line indicate no data retrieved by sediment traps. Grey vertical bars differentiate the summer and winter months.

September 2004 peak-flux event (Fig. 3a; Table 1).

Coccolith flux at 2000 m also increased gradually before a spring/summer maximum in late December of 3.4×10^9 coccoliths m^{-2} d^{-1}, one cup later than at 500 m (Fig. 3b; Table 1). Coccolith flux declined sharply in January, after which a more gradual decline can be inferred before reaching winter lows of 5.01×10^6 coccoliths m^{-2} d^{-1} in May (Fig. 3b; Table 1).

The correlation matrices revealed correlation, to a greater or lesser extent, between all pairs of biogeochemical flux components, and diatom and coccolith flux, at both depths ($p > 0.05$; Table 2). Coccolith fluxes most strongly correlated with CaCO$_3$ fluxes, while diatom fluxes most strongly correlated with BSi fluxes, at both depths. Diatom flux and coccolith flux were weakly correlated with each other at both depths, but particularly at 2000 m (Table 2).

3.4. Diatom flux and seasonality

In total, 64 species or groupings of diatoms were identified between the two trap depths, with 57 diatom taxa at 500 m, and 51 taxa at 2000 m (excluding unidentified pennates and centrics) (Supplementary Tables 2a and 2b). The Shannon-Weaver Equitability index (E$_h$) for diversity and evenness was calculated for diatom assemblages at all sampling intervals, at both depths (Table 1). At 500 m, mean E$_h$ was 0.74, with greatest diversity in February, and lowest in July (Table 1). Mean E$_h$ for the spring/summer period at 2000 m was 0.73, and greatest species diversity was seen in May (Table 1).

Canonical Correspondence Analysis (CCA) was applied to log-transformed fluxes of 19 diatom species, each over 0.5% mean relative abundance at 500 m (Table 3), constrained by two environmental variables (PAR and SST) (Fig. 4a). Axis one accounted for 99.9% of the variation observed, while axis two explained the remainder. Three rough groupings of diatoms were identified, with two species,

Table 2

Correlation matrices between biogeochemical fluxes and diatom /coccolith flux. Values above 0.05 indicate significance.

500 m trap	Mass Flux	BSi flux	CaCO₃ flux	POC flux	Diatom flux	Coccolith flux
Mass Flux	–					
BSi flux	0.97	–				
CaCO3 flux	1.0	0.97	–			
POC flux	1.0	0.96	1.0	–		
Diatom flux	0.79	0.87	0.78	0.78	–	
Coccolith flux	0.97	0.89	0.97	0.97	0.74	–
2000 m trap	Mass Flux	BSi flux	CaCO₃ flux	POC flux	Diatom flux	Coccolith flux
Mass Flux	–					
BSi flux	0.92	–				
CaCO3 flux	0.99	0.86	–			
POC flux	0.94	0.94	0.88	–		
Diatom flux	0.87	0.95	0.80	0.97	–	
Coccolith flux	0.64	0.43	0.71	0.39	0.25	–

Table 3

Annual percentage contribution (Relative Abundance, RA) of diatom and coccolithophore species to total annual flux. (Note: only diatom species > 0.5% annual RA are included, and only coccolithophore taxa seen in two or more cups are included). See Supplementary Tables 2a, 2b, 4a, 4b for complete species listing.

Species	500 m		2000 m
	% flux annual	% flux spring/summer	% flux spring/summer
Fragilariopsis kerguelensis	24.8	21.1	15.3
Azpeitia tabularis	10.8	12.9	5.0
Chaetoceros resting spore	7.2	3.2	5.9
Thalassiosira sp. 1	7.0	10.1	3.4
Thalassiosira lineata	6.0	7.3	2.9
Roperia tesselata	2.9	3.7	1.6
Stellarima microtrias	2.5	3.2	1.3
Nitzschia bicapitata	2.3	3.2	5.9
Thalssiothrix spp.	1.7	1.1	2.4
Rhizosolenia bergonii	1.7	2.0	0.9
Hemidiscus cuneiformis	1.6	2.0	1.1
Shionodiscus oestrupii	1.6	1.6	1.4
Nitzschia sicula var. bicuneata	1.5	2.1	2.2
Shionodiscus frenguellii group	1.3	2.1	0.5
Fragilariopsis doliolus	1.2	1.5	1.0
Thalassiosira lentiginosa	0.8	1.0	0.5
Nitzschia kolaczekii	0.8	1.1	0.7
Chaetoceros vegetative cell	0.7	1.0	8.3
Thalassiosira ferelineata	0.7	0.5	0.8
Emiliania huxleyi	59.3	52.3	78.5
Gephyrocapsa spp. < 3 μm	37.9	43.3	13.0
Calcidiscus leptoporus	1.3	1.9	4.6
Helicosphaera carteri	0.8	1.0	1.7
Syracosphaera spp.	0.2	0.4	0.5
Coccolithus pelagicus	0.2	0.5	0.8
Gephyrocapsa mullerae	0.2	0.3	0.5
Gephyrocapsa oceanica	0.1	0.3	0.4

Fig. 4. Canonical Correspondence Analysis (CCA) of (A) 19 diatom; and (B) 8 coccolithophore taxa from 500 m, constrained by PAR and SST (black lines). Numbers represent sample cups. Dots represent individual species/taxa. Solid lines=ecological groupings; dashed lines=tentative groupings. (A) Diatom taxa. PAR gp.=first grouping, or PAR group; Trans gp.=second grouping, Transition group; Pres gp.=third grouping, Preservation group, as defined in text. Key: A. tab=*Azpeitia tabularis*; CRS=*Chaetoceros* resting spores; CVC=*Chaetoceros* vegetative cells; F. dol=*Fragilariopsis doliolus*; F. kerg=*F. kerguelensis*; H. cun=*Hemidiscus cuneiformis*; N. bic=*Nitzschia bicapitata*; N. kola=*N. kolaczekii*; N. sic=*Nitzschia sicula* var. bicuneata; R. berg=*Rhizosolenia bergonii*; R. tess=*Roperia tesselata*; S. freng. gp.=*Shionodoscus frenguellii* group; S. micro=*Stellarima microtrias*; S. oest=*Shionodiscus oestrupii* ; T. lent=*Thalassiosira lentiginosa*; T. lin=*T. lineata*; T. sp 1=*Thalassiosira* species 1; Thal'thrix=*Thalassiothrix* spp. (B) Coccolithophore taxa.

Thalassiosira ferelineata and *Nitzschia sicula* var. *bicuneata* falling outside of these groupings (Fig. 4a). The first grouping identified correlated most strongly with PAR. Group one contained *Thalassiothrix* spp., *Thalassiosira* sp. 1, *Rhizosolenia bergonii*, *Nitzschia kolaczekii,* and *Fragilariopsis doliolus*, with the *Shionodiscus frenguellii* group tentatively included (Fig. 4a). Combined group one reached maximum abundance peaks during spring and early summer, between September and November, and up to December (Fig. 5). *Shionodiscus frenguellii* group was included as it also displays the early growth pattern of the other group one species. The second grouping identified contained species that reached maximum abundances in late summer and autumn (end of February onwards), but were also present earlier in the season. This grouping was more closely related to SST, and included *Chaetoceros* resting
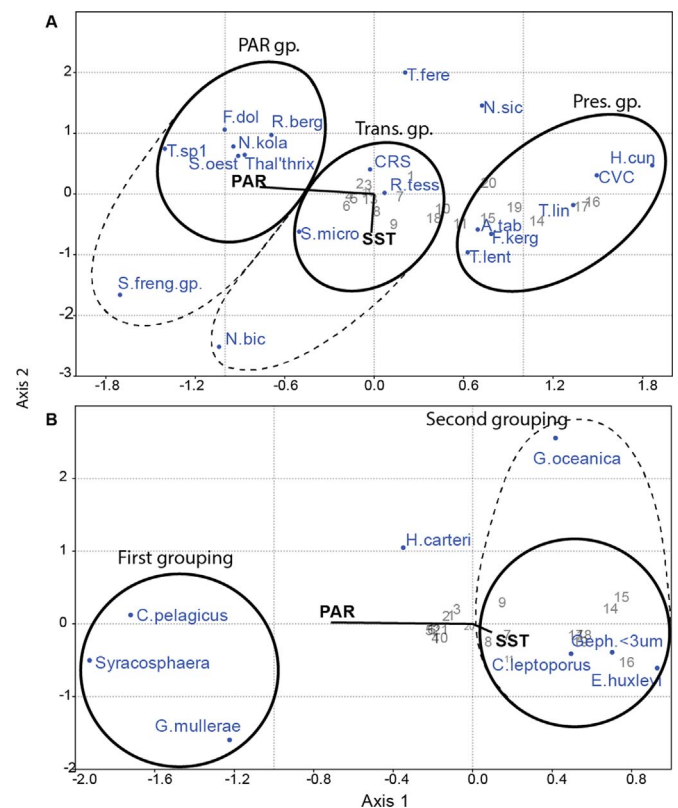
spores, *Stellarima microtrias*, and *Roperia tesselata,* with the speculative inclusion of *Nitzschia bicapitata,* which also displayed high relative abundances in late summer, and in winter (Fig. 4a; Fig. 5). The third grouping identified contained the heavily silicified species *Fragilariopsis kerguelensis, Azpeitia tabularis, Thalassiosira lentiginosa, Chaetoceros* vegetative cells, *T. lineata,* and *Hemidiscus cuneiformis* (Fig. 4a). The group three species tended to occur at maximum abundances at higher SSTs (usually > 10 ºC) and later in the sample
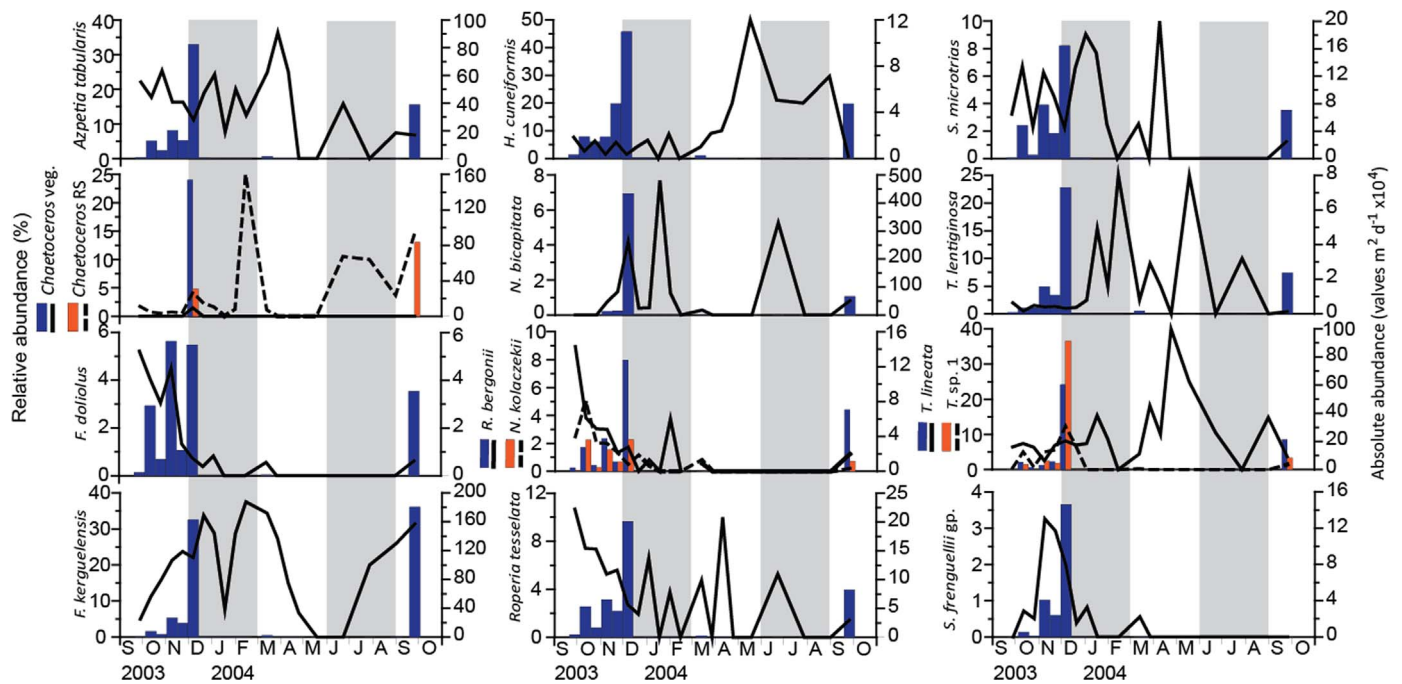
Fig. 5. Relative abundance (%; lines) and absolute abundance (valves m^{-2} d^{-1} × 10^4; bars) at 500 m of 15 diatom taxa of over 1% spring/summer relative abundance. Grey vertical bars differentiate the summer and winter months.

period, but were generally present year-round.

Figs. 5 and 6 show the relative and absolute abundances of the most abundant diatom species, at both depths. Species present throughout, or for most of the year, were *Azpeitia tabularis*, *Fragilariopsis kerguelensis* and *Roperia tesselata*. *Fragilariopsis kerguelensis* was the most abundant diatom in almost every month at 500 m, comprising 25% of mean annual abundance (Table 3). During the spring/summer period, *F. kerguelensis* was 21% and 15% of total diatoms captured at 500 m and 2000 m, respectively (Table 3). Seasonally, *F. kerguelensis* made up a greater portion of the diatoms captured during the mid/late summer period (~December to February), although this trend was more pro-

nounced at 500 m than at 2000 m (Figs. 5 and 6). *Azpeitia tabularis* also constituted a significant fraction of diatoms observed year-round at both depths. At 500 m, *A. tabularis* averaged 13% mean relative abundance during the spring/summer period, and reached 39% abundance at its peak in March (Fig. 5). *Azpeitia tabularis* averaged 5% across the spring/ summer period at 2000 m (Fig. 6). Maximum relative abundances of *Roperia tesselata* at both 500 m and 2000 m were seen at the beginning of the sampling period in September (11% and 12%, respectively) (Figs. 5 and 6). *Roperia tesselata* relative abundances declined after September at both depths, with fluctuating abundances for the remainder of sampling (Figs. 5 and 6).
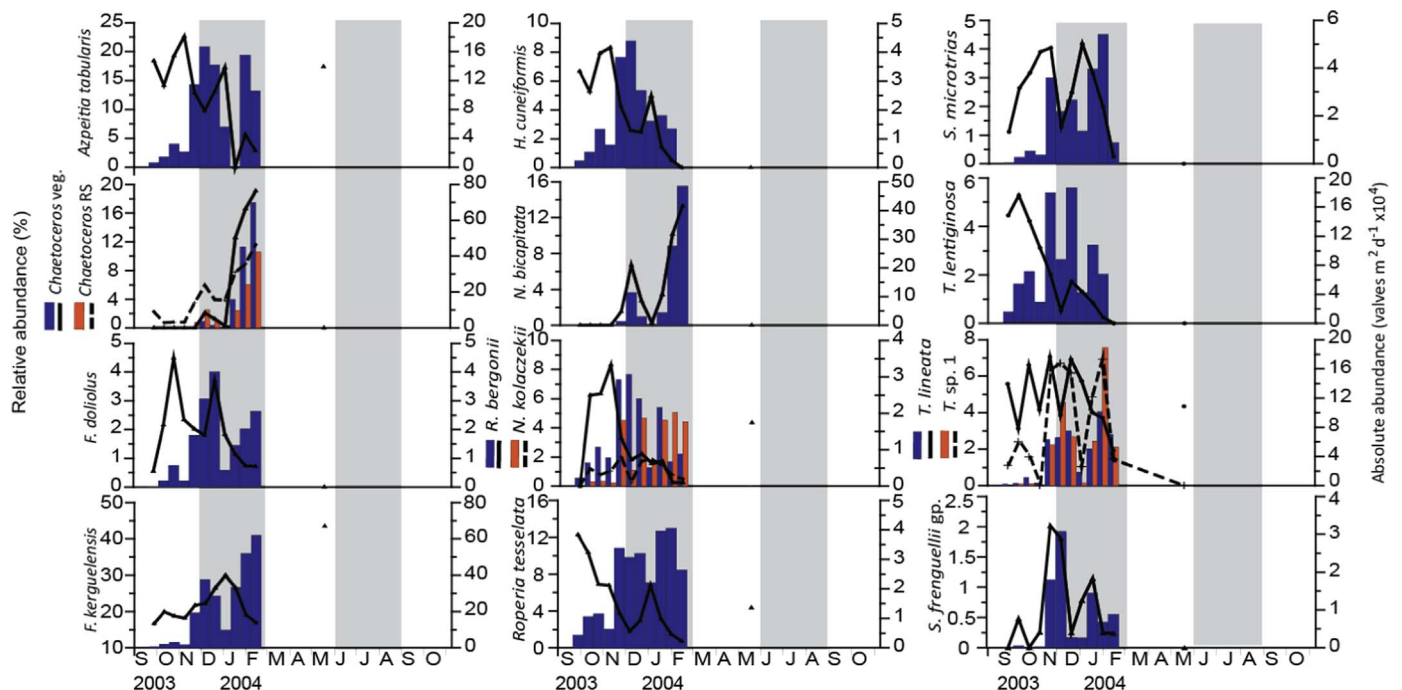

Fig. 6. Relative abundance (%; lines) and absolute abundance (valves m^{-2} d^{-1} × 10^4; bars) at 2000 m of 15 diatom taxa of over 1% spring/summer relative abundance. Grey vertical bars differentiate the summer and winter months.

The species present during the spring/summer period, but absent or exhibiting low abundances during the autumn and winter months were *Fragilariopsis doliolus, Nitzschia kolaczekii, Rhizosolenia bergonii, Thalassiosira* species 1, and *Shionodiscus frenguellii* group (Fig. 5). *Chaetoceros* vegetative cells were present only in one cup in early December at 500 m, but appeared slightly later at 2000 m, although they constituted a substantial 20% of relative abundances in February at 2000 m.

Several diatom species appeared at low abundances or were absent early in the year, but were present during the autumn/winter months. *Hemidiscus cuneiformis* was present throughout the spring/summer period at ~5% relative abundance, but was significant in winter assemblages, peaking to 50% relative abundance in May at 500 m (Fig. 5). At 2000 m, highest *H. cuneiformis* abundances of approximately 8% were seen in November (Fig. 6). *Thalassiosira lineata* was present throughout the sampling period at 500 m, although highest abundances occurred in late April (Fig. 5). To a lesser extent, at 2000 m *T. lineata* averaged only 3% relative abundance in the spring/summer period, but was almost 5% of diatoms present in winter (Fig. 6).

Chaetoceros resting spores contributed little to total flux between September and early December at 500 m (~1%), but peaked in cup 11 at 25% of diatom relative abundance. Annually, *Chaetoceros* resting spores averaged 7.2% of diatom assemblages (Table 3). *Chaetoceros* resting spores were also present in winter, and towards the end of the sampling period (June to September) (Fig. 5). *Thalassiosira lentiginosa* followed a similar late-blooming trend at 500 m, with a peak abundance of 25% in February (Fig. 5). At 2000 m, *Chaetoceros* resting spores and *T. lentiginosa* comprised a relatively small component of the diatom fluxes in the spring/summer period (6% and 0.5% of relative abundance, respectively).

3.5. Coccolithophore flux and seasonality

In total, eleven coccolithophore species or groups were found in the sediment traps. *Emiliania huxleyi* dominated coccolithophore assemblages at both depths, representing 59% of total annual coccolithophore flux (Table 1).

A CCA was applied to the eight most abundant coccolithophore taxa observed in this study, constrained by PAR and SST (Fig. 4b). Axis one revealed 93% of variation in the dataset. The CCA indicated two major groupings of coccolithophore taxa (Fig. 4b). The first grouping contained three taxa: *Coccolithus pelagicus, Syracosphaera* spp.*,* and *Gephyrocapsa muellerae*. The species in this grouping exhibited peak abundances in spring and summer, with lower abundances later in the sampling period, with the exception of the more complex pattern shown by *G. muellerae* (Fig. 7). The second grouping of coccolithophore taxa revealed by the CCA was composed of *Emiliania huxleyi, Gephyrocapsa* spp. < 3 μm, and *Calcidiscus leptoporus*. The species in the second grouping either exhibited peak abundances in spring/summer and remained abundant throughout the sampling year, or were most abundant during the autumn/winter period (*E. huxleyi, C. leptoporus,* and *Gephyrocapsa* spp.; Fig. 7). Two species, *Helicosphaera carteri* and *Gephyrocapsa oceanica,* did not appear to fit with either grouping.

The relative abundance of *Emiliania huxleyi* was stable throughout the sampling period. *Emiliania huxleyi* represented 52%, and nearly 80% of spring/summer coccolith flux at 500 m and 2000 m, respectively (Table 3). Maximum *E. huxleyi* abundances occurred in April at 500 m, at which point it dominated coccolith flux at 94% of total coccolith abundance (Fig. 7). At 2000 m, the maximum peak of *E. huxleyi* occurred in December, representing 90% of coccolith abundance (Fig. 8).

Gephyrocapsa spp. < 3 μm averaged 43% of spring/summer coccolith fluxes at 500 m, but were less abundant at 2000 m, at only 13% of coccolith fluxes (Table 3). Peak abundances occurred in November at 500 m, where *Gephyrocapsa* spp. < 3 μm comprised 57% of the coccolithophore assemblage. Abundances of this group were lower in the autumn/winter period, but remained a significant fraction of the fluxes (Fig. 7). Peak *Gephyrocapsa* spp. < 3 μm abundances of about 50% of all coccoliths at 2000 m were seen in May (Fig. 8). *Calcidiscus leptoporus* and *Gephyrocapsa oceanica* showed similar trends in abudance as *Gephyrocapsa* spp., whereby both species appeared most abundant in the 500 m sediment trap in late summer/early autumn (Figs. 7 and 8) at both depths. *Calcidiscus leptoporus* reached a maximum 13% of the coccolithophore assemblage in February, but was a small contributor (av. < 4%) to coccolith fluxes for the rest of the sampling period (Fig. 7).

Syracosphaera spp. and *Coccolithus pelagicus* exhibited highest relative abundances in spring, with peaks in September and October, respectively (Fig. 7), and lower or fluctuating abundances for the rest of the sampling year. *Gephyrocapsa muellerae* was found at highest relative abundances in winter, but peaked in absolute abundance in late spring/early summer at 500 m (Fig. 7).

4. Discussion

4.1. Magnitude and composition of the particle fluxes

The annual TMF in the 500 m trap (17 g m^{-2} y^{-1}) was within the range of previous flux measurements at 1000 m at the 47°S site (15 ± 3 g m^{-2} y^{-1} at 1000 m; Rigual-Hernández et al., 2015b; Trull et al., 2001c). Moreover, annual TMF at 500 m was of the same order of magnitude as, though slightly higher than, fluxes measured in the western Pacific and New Zealand sectors of the SAZ (11.5 g m^{-2} y^{-1} at 1000 m (Honjo et al., 2000) and 14.9 g m^{-2} y^{-1} at 1500 m (Nodder et al., 2016), respectively). The similarity between fluxes recorded at 500 m (present study) and the fluxes recorded at 1000 m (Honjo et al., 2000; Nodder and Northcote, 2001) indicate that the particle fluxes experienced little change between the base of the mixed layer and the mesopelagic zone (~1000 m) (i.e. the deep twilight). Annual TMF was not calculated for the 2000 m trap, as only cups 1−11 and 17 contained enough material for analysis. When only these first 11 sampling cups representing the spring/summer period were taken into account, TMF at the 2000 m trap was higher than at the 500 m trap (103 vs. 60.5 mg m^{-2} d^{-1}, respectively) (Table 1). Trapping efficiency is often greater at depth due to lower current speeds and greater consolidation of aggregates (Scholten et al., 2001; Yu et al., 2001), potentially explaining the higher fluxes at the 2000 m trap. Input of resuspended sediment into deep sediment traps has been reported in pelagic systems (e.g. Treppke et al., 1996). The potential lithogenic transport and input from the Tasmanian coast via the Tasman Outflow (EAC derived; Herraiz-Borreguero and Rintoul, 2011) has been considered previously (Findlay, 1998; Findlay and Giraudeau, 2000; Rigual-Hernández et al., 2016b). Yet, evidence from lithogenic fluxes calculated from the initial SAZ project sediment trap deployment at 47°S (1997–1998) were very low: 0.66 g m^{-2} y^{-1} at 2000 m (Trull et al., 2001a), suggesting that the influence of resuspended sediments can be considered negligible in this study.

Biogeochemical fluxes at 47°S were carbonate-rich (> 70% annual TMF; Table 1) and silicate-poor, confirming previous regional microplankton investigations where live assemblages were dominated by non-siliceous taxa (de Salas et al., 2011; Kopczyńska et al., 2001). Coccolith flux to both depths was over three orders of magnitude greater than diatom flux. Although this study did not calculate the specific contribution of coccoliths to the carbonate component of fluxes captured in the traps, the very high correlation between coccolith and CaCO$_3$ fluxes (Table 2) suggest that coccoliths were likely an important contributor to the carbonate fraction. Likewise, diatom flux was strongly correlated with BSi flux, again suggesting that diatoms were an important component of BSi fluxes at both depths (Table 1).
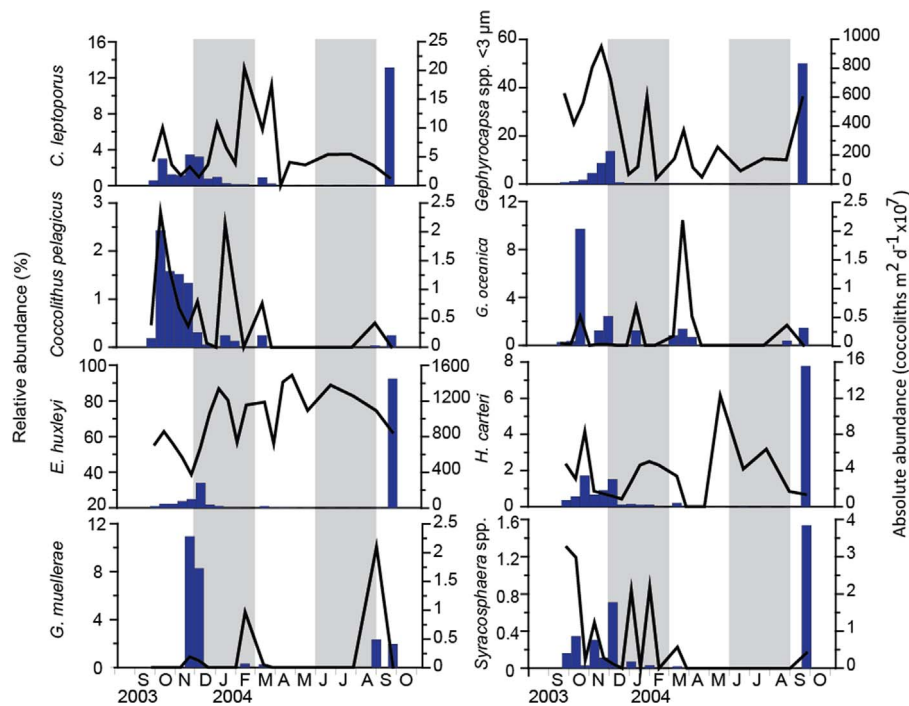
Fig. 7. Relative flux contributions (%; lines) and absolute abundance (coccoliths m^2 d^{-1} ×10^7; bars) of eight major coccolithophore taxa across the sampling year at 500 m. Grey vertical bars differentiate the four seasons. Missing cup 12 not indicated.

Foraminifera and pteropods are also known to be important contributors to Southern Ocean CaCO$_3$ export (Schiebel, 2002; King and Howard, 2005; Howard et al., 2011; Roberts et al., 2011), but were not considered in this study. However, both pteropod and foraminifera fluxes have been previously documented in sediment traps from the region (Howard et al., 2011 and King and Howard, 2003, respectively).

The BSi: PIC molar ratio at this site was «1 (Table 1), placing it within the "carbonate ocean" defined by Honjo et al. (2008), as opposed to zonal systems further south where particle fluxes are diatom-dominated (i.e. "silica ocean"). The annual POC flux measured at 500 m at 47°S (1.1 g m^{-2} yr^{-1}) was similar to those reported in previous 1000 m depth deployments at the same site (0.9–1.4 g m^{-2} yr^{-1}; Rigual-Hernández et al., 2015b; Trull et al., 2001c), and in the SAZ of the western Pacific sector (1.0 g m^{-2} yr^{-1}; Honjo et al., 2000). The annual POC flux values at 500 m were similar to the global average of 1.4 g C m^{-2} d^{-1} (normalised to 2000 m; Lampitt and Antia (1997)),
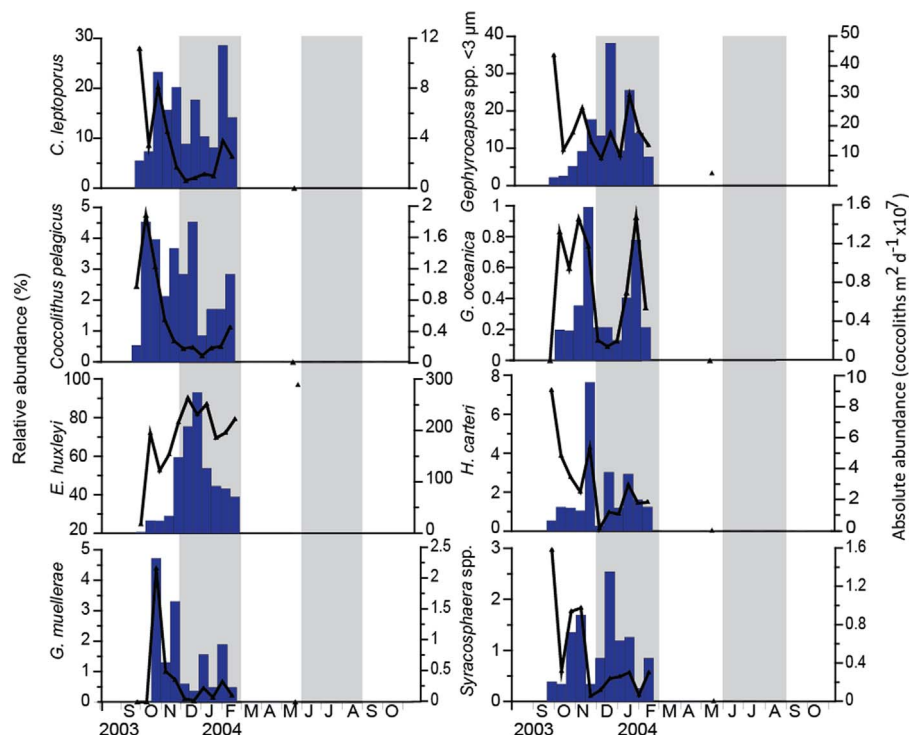

Fig. 8. Relative flux contributions (%; lines) and absolute abundance (coccoliths m^2 d^{-1} ×10^7; bars) of eight major coccolithophore taxa across the sampling year at 2000 m. Grey vertical bars differentiate the four seasons. No data available in March and April, and from June to October. Data from cup 17 (May) is shown as a data point on each plot.

which highlights the importance of this region for carbon sequestration despite its relatively low algal biomass accumulation (Bowie et al., 2011). In this study POC flux was not normalised due to the lack of a full annual data series from this study, and would be slightly lower if normalised to 2000 m.

4.2. Temporal dynamics of particle fluxes

Total Mass Flux (TMF) peaked in December in both the 500 and 2000 m traps, and again in February at the 2000 m trap only (Fig. 2a and b). Maximum TMF occurred one month prior to peak chlorophyll-*a* concentrations, and one sampling interval later than maximum PAR (Fig. 2a). Peak Chl-*a* represents the time at which plankton abundances are greatest, and yet TMF in the sediment trap peaked and began to decline before the Chl-*a* maximum. Although speculative, if the sediment traps were capturing material from an earlier-blooming patch of ocean due to lateral transport, then maximum trap abundances could appear to occur before peak Chl-*a* was measured. The second TMF peak at 2000 m occurred one cup later than maximum Chl-*a*, but was not observed in the 500 m trap, again suggesting the capture of a bloom upstream of the mooring site at 2000 m.

Both diatom and coccolith fluxes peaked simultaneously in December (Fig. 3), and subsided before peak Chl-*a* concentration in surface waters (Fig. 2). This observation is surprising, as diatoms typically bloom before coccolithophores in temperate (e.g. Margalef, 1978; Rigual-Hernández et al., 2013; Thunell et al., 1996) and polar regions (Alvain et al., 2008). The simultaneous peaks in biogeochemical flux components and both diatoms and coccoliths could be due to the co-sedimentation of material into the sediment traps, caused by aggregation of material (Rigual-Hernández et al., 2015b), with this speculation consistent with the correlation matrix outcomes.

The bulk of oceanic POC export in many pelagic ecosystems often occurs in the form of aggregates, which can be clusters of cells and particles ballasted by lithogenic material and phytoplankton remains and/or zooplankton faecal pellets (Honjo et al., 2008). Coccolith-ballasted aggregates are denser and tend to fall faster through the water column than diatom-ballasted aggregates (Klaas and Archer, 2002; Iversen and Ploug, 2010). Coccoliths can be "scavenged" by aggregates (De La Rocha and Passow, 2007; Iversen et al., 2010), enhancing transport speed (Iversen and Ploug, 2010). During times of high productivity (e.g. September to December at 500 m), rapid aggregate or faecal pellet formation and scavenging of smaller particles could lead to the simultaneous peaking of coccoliths and diatoms in sediment traps, as previously suggested by Rigual-Hernández et al. (2015b). The correlation between all biogeochemical components, and both phytoplankton groups shown in the correlation matrix (Table 2) lends further support to the suggestion of co-sedimentation of material, and explains why the two groups appear to flourish at the same time in sediment traps.

Particle sinking speed was not estimated in this study, however, the peaks in TMF at both 500 m and 2000 m depth that occurred in December were presumed to represent the capture of the same bloom material. For this to be the case, sinking speeds of ~107 m d^{-1} are sufficient for the 14 d capture interval in the spring/summer period. A sediment trap study in the Australian sector of the PFZ found POC sinking rates of up to 850 m d^{-1} (Ebersbach et al., 2011), hence the estimated ~107 m d^{-1} is plausible. At 47°S, however, Rigual-Hernández et al. (2016b) calculated particle settling speeds of only 20 m d^{-1} between 1000 m and 2000 m depth. These latter settling speed estimates at the deeper depths did not investigate the type or form of exported particles. Particles packaged within faecal pellets, for example, will fall much faster than amorphous aggregates (Ebersbach et al., 2011). In order for particles to travel the estimated ~107 m d^{-1} required in the present study, aggregated faecal pellets would have been the likely export particle form. The state of particles captured in this study's sediment traps was not noted due to post-collection

modification of material, however, it is possible that faecal pellets were also the main form of particle packaging and settling in this study.

Fluxes between autumn and winter (March–August, 500 m) were uncharacteristically low in comparison to a multi-year trapping study at 800 m at the same site (Rigual-Hernández et al., 2015b), while fluxes registered in September 2004 during the peak-flux event were atypically high. A potential explanation is that the trap opening clogged in mid-February, resulting in low capture for the remainder of the year, until the built-up material presumably fell, all at once, into the final cup. If this was the case, then estimates of annual TMF are still valid, as the material captured in the peak-flux event represents that of the entire late summer to winter period. However, it may not be meaningful to analyse winter flux seasonality, thus discussion hereafter focuses on the spring/summer capture period.

4.3. Coccolith and diatom fluxes

The coccolith flux values in this study are some of the highest recorded in sediment traps deployed in the Southern Ocean. By way of comparison, a study by Ternois et al. (1998) in the Indian sector of the Southern Ocean (50°S, 68°E), within the PFZ, documented coccolith fluxes four orders of magnitude lower (4.7×10^7 m^{-2} yr^{-1}), despite trapping at a similar latitude. Contrarily, studies on living coccolithophore assemblages in the New Zealand sector indicated the highest concentrations of coccolithophores within the PFZ, and lowest within the SAZ (Malinverno et al., 2015, 2016). Coccolith concentrations are seasonally so high in the Southern Ocean, particularly near the Subantarctic Front, that the region has been termed the "Great Calcite Belt" (Balch et al., 2011, 2016).

Coccolith fluxes in this study were similar to findings at more temperate sites. Broerse et al. (2000) calculated 4.4×10^{11}, and 1.4×10^{11} coccoliths m^{-2} yr^{-1} in sediment traps deployed in the subtropical (34°N) and temperate (48°N) northeast Atlantic, respectively. Ziveri et al. (2000) captured coccolith fluxes from traps placed in the northeast Atlantic (48°S) of 1×10^{10} coccoliths m^{-2} y^{-1}. In the tropical Panama Basin (2°S–8°N), traps deployed by Steinmetz (1994) recorded coccolith fluxes of 1.2×10^{11} m^{-2} yr^{-1}, and 3.3×10^{11} m^{-2} yr^{-1}. The coccolith fluxes found in the SAZ, south of Australia, appear to represent abundances transitional between those seen in polar or warmer temperate regions.

Annual diatom valve fluxes at 500 m in the present study (2.3×10^8 valves m^{-2} yr^{-1}) are in agreement with the diatom flux estimate of 0.3×10^8 valves m^{-2} yr^{-1} at 1000 m at the same site (Rigual-Hernández et al., 2015b). The latter authors' findings suggest little silica dissolution below the mixed layer, and that annual diatom export at 47°S in the SAZ, south of Australia, is relatively constant.

The temporal flux observations from the 47°S traps are in line with previous studies globally and regionally. Low diatom fluxes are typical of low-productivity areas of the carbonate ocean, such as much of the SAZ, including the present study region (Trull et al., 2001b; Honjo et al., 2008). Diatom growth in the SAZ is thought to be limited by low iron and silicic acid availability (Hutchins et al., 2001; Leblanc et al., 2005), as well as light limitation due to the deep mixed layer (Rintoul and Trull, 2001). Coccolithophores are not Si-dependent, and can tolerate low nutrient concentrations (Balch, 2004). The southernmost extent for coccolithophore growth appears to be at around 2 °C (Gravalosa et al., 2008). In the Australian sector, with the exception of *Emiliania huxleyi*, coccolithophore abundances decrease south of the SAZ, and are not found below the Polar Front (Findlay and Giraudeau, 2000). The distribution of *E. huxleyi* is more complex, forming a monospecific assemblage south of the Polar Front, before abundances halt polewards of ~60°S (Nishida, 1986; Findlay and Giraudeau, 2000). In the Indian sector of the STZ and PFZ, the high abundances of the ubiquitous *E. huxleyi* have been attributed to the inability of diatoms to take advantage of the available nutrients (Patil et al., 2014). It is likely that a similar situation occurs in the Australian

sector of the SAZ, whereby coccolithophores and other phytoflagellates are able to capitalise on available nutrients, hence the low diatom abundances reported in both live (Kopczyńska et al., 2007) and sediment trap samples (this study; Rigual-Hernández et al., 2015b).

4.4. Diatom assemblage composition and seasonality

The diatom assemblage at 47°S was consistent with Subantarctic assemblages influenced by Subtropical waters, as previously reported from studies focused on both live assemblages (e.g. Kopczyńska et al., 2001; Kopczyńska et al., 2007; De Salas et al., 2011; Olguín et al., 2011; Assmy et al., 2013) and more regionalised seafloor sediment distributions (e.g. Armand et al., 2005; Crosta et al., 2005; Romero et al., 2005a, 2005b; Rigual-Hernández et al., 2016b). The influence of warmer waters relative to the trap location was demonstrated via moderate to rare occurrences of diatom taxa such as *Thalassiosira lineata, Fragilariopsis doliolus, Nitzschia* spp.*, Hemidiscus cuneiformis*, and isolated occurrences of *Cocconeis* spp. and *Diploneis* spp. (Table 3). The Zeehan Current, which flows from coastal South Australia, and southwards along western Tasmania, is a possible source of warm water species input, in conjunction with the East Australia Current (EAC)-derived Tasman Outflow (Herraiz-Borreguero and Rintoul, 2011). Thus, the possibility of diatom species input from the Tasmanian shelf is not unlikely, and previous studies have speculated on the influence of Tasmanian waters on sediment trap assemblages at the same site (Rigual-Hernández et al., 2016b). Seafloor sediment assemblages reported elsewhere resembled the species compositions observed in the traps more closely than in surface water studies, with high sediment abundances of *Azpeitia tabularis* (Romero et al., 2005a, 2005b) and *Fragilariopsis kerguelensis* (Crosta et al., 2005). Some subtropical species occurred at 47°S, including *Fragilariopsis doliolus, Roperia tesselata, Thalassiosira symmetrica, Hemidiscus cuneiformis* and *Shionodiscus oestrupii* (formerly *Thalassiosira oestrupii*) (Crosta et al., 2005; Romero et al., 2005a, 2005b). Lower diatom assemblage diversity in winter cups was likely a product of the low sample sizes (Table 1; Supplementary Tables 2a and 2b).

The results of the CCA performed on the diatom fluxes revealed three rough ecological groupings found within sediment traps: the PAR (first group), Transition (second group), and Preservation (third group) species, which were collectively plotted by way of comparison with the current understanding of live diatom succession (Fig. 9b). These ecological groupings are consistent with the theories of diatom succession proposed by both Guillard and Kilham (1977) for the Southern Ocean, and Quéguiner (2013) for the Permanently Open Ocean Zone (POOZ) and the PFZ, summarised in Fig. 9a. Diatom succession schemes for the Southern Ocean identify two different "groups" of diatoms, forming three different assemblage stages. Early diatom assemblage succession in the POOZ and PFZ is generally dominated by fast-growing, lightly silicified species (i.e. opportunistic or r-strategists) that take quick advantage of the increased light in spring- the "group 1" species (Quéguiner 2013), forming the stage 1 assemblage (Guillard and Kilham, 1977) (Fig. 9a). As "group 1" species decline, they are overtaken by "group 2" species, which are slower-growing, large, and more heavily silicified, with a more persistent growth strategy. High abundances of "group 2" species represent stage 3 of diatom succession. Stage 2 occurs at the point junction between "group 1" and "group 2" species, and represents the most diverse stage of diatom succession (Guillard and Kilham, 1977).

Diatoms, as well as other plankton groups, preserved within sediment traps, reflect live assemblage succession after the filter of transformational processes, which occur during particle sinking, have taken place. These transformational processes include lateral transport, particle repackaging and dissolution, and as such, sediment traps are likely to provide an altered chronology of species succession and relative abundances to live assemblage studies. Fig. 9b highlights the apparent succession of the three ecological groupings identified by the
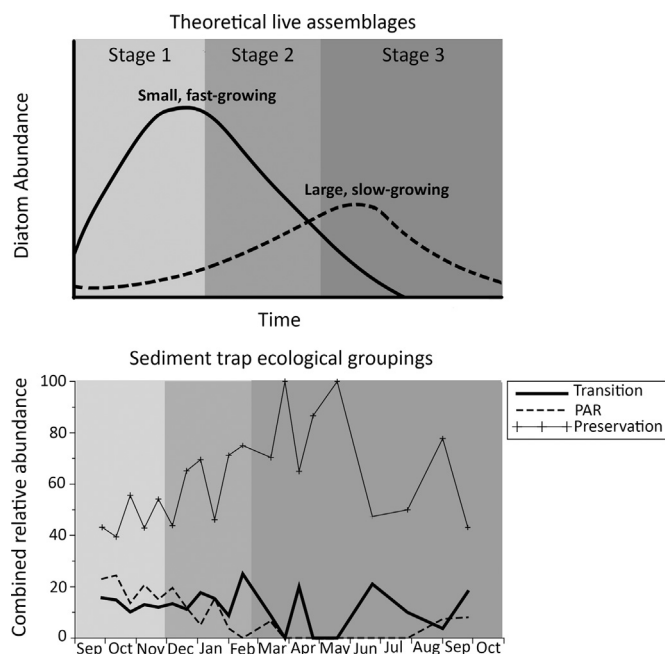

Fig. 9. Schematic illustrating theoretical diatom succession in live assemblages and sediment traps across a year in the SAZ (adapted from Guillard and Kilham (1977) and Quéguiner (2013)). (A) Theoretical live assemblage succession of diatom groups: Stage 1 (light grey)=assemblage type dominated by small, fast-growing diatoms; Stage 2 (mid grey)=transitional assemblage type with high-diversity diatom assemblage; Stage 3 (dark grey)=assemblage dominated by large, slow-growing diatoms. (B) Combined relative abundances of diatoms grouped into PAR, Transition and Preservation groups in this study, across sampling year, as per groups indicated on Fig. 4.

CCA. In 9b, the Preservation ecological grouping appears abundant year-round, and particularly in winter. Of the other two groupings, the PAR group reaches maximum abundances in early spring (during the theoretical stage 1), and is overtaken by the Transition grouping in summer (theoretical stage 2). During this theoretical stage 2 within the sediment trap assemblages, diversity indices were highest (Table 1), as per Guillard and Kilham (1977). In sediment trap stage 3, the heavily silicified Preservation grouping dominated diatom assemblages, with a sporadic presence of Transition species.

The PAR group identified from sediment trap assemblages was analogous to the stage 1 of diatom succession identified by Guillard and Kilham (1977) (Fig. 9a). This is supported by the correlation between PAR and the PAR group species in the CCA (Fig. 4a). *Chaetoceros* vegetative cells are commonly cited as the quintessential early-blooming species characteristic of this growth pattern (Smetacek et al., 2004; Assmy et al., 2013; Boyd, 2013). While the vegetative cells of *Chaetoceros* were almost absent at 500 m, they made up on average 8% of assemblages at 2000 m, appearing in late summer (December to February). *Chaetoceros* spp. are opportunistic and form localised blooms (Assmy et al., 2013), which could explain the appearance of *Chaetoceros* vegetative cells in the deeper trap alone if the 500 m and 2000 m traps were sampling from different surface ocean patches.

Of the PAR group species, *Fragilariopsis doliolus, Rhizosolenia bergonii* and *Nitzschia kolaczekii* typically inhabit more temperate waters (Hasle and Syvertsen, 1997). *Fragilariopsis doliolus* and *R. bergonii* exhibit persistent, but low, abundances within the northern SAZ (Zielinski and Gersonde, 1997). The light silicification of "group 1" species means that they are likely to be dissolved or fractured via predation in the water column, leaving a much smaller record in sediments than reflects their live abundances (Romero et al., 2000; Romero et al., 2005a, 2005b). As a result, the "group 1" diatom signal may be reduced or possibly invisible in sediment trap and seafloor sediment studies compared to live observations. In addition to this, sediment trap and seafloor sediment studies are likely to find that

"group 1" species appear later in the season than expected, simply due to the time elapsed between photic zone production and trap capture or sedimentation (Fig. 9a; b).

The second successional grouping, the Transition group, was characterised by the appearance of *Chaetoceros* resting spores (CRS) within the sediment traps at 500 m and 2000 m. CRS were present in spring, but appeared in significant numbers in late summer as the bloom subsided (February and January; 500 m and 2000 m respectively) (Figs. 5 and 6). CRS formation is triggered by declining environmental conditions, particularly nitrogen limitation, but also iron, silica and light limitation, such as occurs later in a bloom (e.g. Leventer, 1991; Assmy et al., 2013). Resting spore formation represents the transition from the fast-growing PAR group towards an assemblage characterised by slower-growing, heavily silicified species (Quéguiner, 2013; Boyd et al., 2013; Guillard and Kilham, 1977) (Fig. 9). Two centric species, *Stellarima microtrias* and *Roperia tesselata*, appeared within the Transition group. Both of these species were present throughout the spring sampling period, but reached maximum abundances in April before declining to almost zero abundances during the rest of the sample interval (Fig. 5). While *R. tesselata* is commonly reported from the Subantarctic, *S. microtrias* is endemic to the colder waters of the Southern Ocean (Hasle and Syvertsen, 1997). This is potentially due to the transport of cooler water northwards crossing the SAF (Rintoul and Trull, 2001), carrying this species into the study area. *Nitzschia bicapitata* was also tentatively placed within the Transition grouping, as it showed peak abundances within spring and summer, but was also present in one winter month (Fig. 5).

The third diatom grouping observed was named the Preservation group, containing almost exclusively large, well-silicified diatoms, with persistent year-round abundances, particularly abundant in the autumn and winter months from March onwards. The Preservation group archetype was *Fragilariopsis kerguelensis*, the most abundant and widespread diatom in the surface sediments of the Southern Ocean (Crosta et al., 2005). It was the most abundant diatom found in sediment traps at both depths, and present year-round, (Figs. 5 and 6; Table 3). *Fragilariopsis kerguelensis* exhibits a persistent strategy (slow growing but present season-round), and is considered to sink silica rather than carbon due to its thick, grazing and dissolution-resistant frustule (Assmy et al., 2013). Despite being abundant in traps, *F. kerguelensis* was rare in live assemblages at latitudes north of 53.7°S (Kopczyńska et al., 2007). The relative rarity of this species in surface waters compared to sediment traps points to selective enhancement of abundances due to the dissolution of lighter species, as appears the case with all of the Preservation group species.

Other preservation group diatoms included *Azpeitia tabularis*, *Thalassiosira lentiginosa*, *T. lineata,* and *Hemidiscus cuneiformis*; each considered heavily silicified and dissolution resistant species that were well preserved in the 47°S sediment traps. *Azpeitia tabularis* and *H. cuneiformis* are most abundant in subtropical waters, however *A. tabularis* is considered cold tolerant and is abundant within sediments in the SAZ (Romero et al., 2005a, 2005b). The strong presence of *H. cuneiformis* is additional evidence for potential warm, coastal water input from the north to the 47°S site, as this species tends to be associated with more saline, oligotrophic water masses (Romero et al., 2005a, 2005b). *Thalassiosira lentiginosa* is a widespread, open ocean species endemic to the Southern Ocean (Zielinski and Gersonde, 1997), and the large valves of this species were often found intact even in poorly preserved samples. The preservation group in this study can be considered akin to the "group 2" assemblage proposed by Quéguiner (2013), heralding stage 3 of diatom bloom evolution (Guillard and Kilham, 1977).

The diatoms that did not appear to sit within any grouping were *Thalassiosira ferelineata,* and the *Shionodiscus frenguellii* group. It is possible that the chosen environmental variables, SST and PAR, cannot adequately explain the abundance patterns of any of these species, and

that other variables are in play, such as nutrient availability and/or zooplankton grazing.

4.5. Coccolithophore assemblage composition and seasonality

The coccolithophores recovered from sediment traps at 47°S were similar to the *Emiliania huxleyi*-dominated assemblage observed by Findlay and Giraudeau (2000) taken from live samples at the same site.

The CCA performed on the coccoliths found in this study revealed two major ecological groupings. The first grouping contained the taxa *Coccolithus pelagicus, Syracosphaera* spp., and *Gephyrocapsa muellerae*, and appeared more strongly correlated with PAR than the second grouping (Fig. 4b). Both *C. pelagicus* and *Syracosphaera* spp. comprised more of the coccolithophore assemblage within the spring/summer period, and were largely absent during the autumn and winter months. This pattern was less distinct with *G. muellerae*, which displayed sporadic peaks in abundance between periods of absence within the traps (Fig. 7). Despite the incomplete record, the early-peaking trend of the first grouping species was more pronounced at 2000 m, with all three taxa exhibiting highest abundances in September or October, before declining to low winter abundances. Contrary to the apparent seasonal succession recorded in the traps, *Syracosphaera* spp. tend to be K-selected in other settings of the world's oceans, often reaching maximum abundances later in the productive season than more opportunistic coccolithophores (Broerse et al., 2000; Dimiza et al., 2008). In the Australian sector, *Syracosphaera* spp. were described as preferring warmer waters, and were not found live south of 49°S (Findlay and Giraudeau, 2000). Though speculative, the intrusion of warmer water filaments from the north from earlier-blooming coccolithophore populations could have resulted in the early-blooming appearance of *Syracosphaera* spp. captured by these sediment traps. In contrast to the latter species, both *C. pelagicus* and *G. muellerae* exist preferentially in cooler waters (Findlay and Giraudeau, 2000).

The second grouping revealed by the CCA included the three most abundant taxa found in sediment traps, with a preference for cooler waters: *E. huxleyi, Gephyrocapsa* spp. < 3 µm, and *C. leptoporus*, with the tentative inclusion of *G. oceanica* (Fig. 4b). The sharp rise in small *Gephyrocapsa* spp. in late spring was followed by the rise in *C. leptoporus* and *E. huxleyi* between summer and early autumn, and the subsequent assemblage dominance of *E. huxleyi* for the remainder of the year. The ubiquitous cosmopolitan *E. huxleyi* is considered the most abundant coccolithophore species at high latitudes in both hemispheres (e.g. Gravalosa et al., 2008; Saavedra-Pellitero et al., 2014; Winter et al., 2014).

Emiliania huxleyi can be broadly defined as a R-selected, opportunistic species that exhibits a high growth rate compared to other coccolithophore species (Tyrrell and Merico, 2004). High *E. huxleyi* concentrations are a common feature in the Subtropical, Subantarctic, and Polar Fronts (Balch et al., 2011). Although the factors selecting for *E. huxleyi* blooms are still unclear, the development of this species seems to be favoured by water column stability, high incident irradiance, and relatively low nutrient concentrations (Iglesias-Rodríguez et al., 2002). Indeed, *E. huxleyi* blooms in high latitude systems are often associated with moderate stratification of the water column and take place within a few weeks of the summer solstice in high latitude systems of both hemispheres (Balch, 2004). Our results agree well with this pattern as maximum of *E. huxleyi* were registered in December coinciding with both the austral summer solstice and a relatively stratified water column. Several morphotypes of this species exist, though they were not discriminated in this study, as limited material was available for coccolith analysis, and thus only light microscopy was undertaken (see Section 2.4). However, a study by Cubillos et al. (2007) identified *E. huxleyi* morphotypes in the Australian sector of the Southern Ocean, finding the overcalcified "type A" dominant within the SAZ, and replaced by lesser-calcified morpho-

types south of the SAF. Type A *E. huxleyi* coccoliths were likely the main morphotype captured in the present study.

Gephyrocapsa spp. < 3 μm were the next most abundant coccolith grouping following *E. huxleyi*, making up 37.9% mean relative abundance at 500 m, while the remaining species observed each accounted for less than 2% of total coccoliths (Table 3). *Gephyrocapsa* spp. < 3 μm are indicative of high productivity regions such as areas of upwelling (Andruleit et al., 2003). *Gephyrocapsa* spp. < 3 μm respond quickly to nutrient input, and are considered R-selected in strategy (Dimiza et al., 2008), which could explain the greater abundances of *Gephyrocapsa* spp. < 3 μm observed in the late spring/early summer period. *G. oceanica,* like the small *Gephyrocapsa* spp., are also considered R-selected (Dimiza et al., 2008), which lead to the expectation that it would peak earlier in sediment trap assemblages. While it appeared in the summer period, maximum abundances of *G. oceanica* occurred in autumn, hence its inclusion within the second coccolithophore grouping.

Calcidiscus leptoporus represented a small (usually < 10% mean relative abundance) but omnipresent component of coccoliths fluxes throughout the sampling period, at both depths (Fig. 6). This species tends to inhabit cool, nutrient rich waters (Boeckel et al., 2006). Like *E. huxleyi*, several morphotypes of this species exist, however, they were not identified in this study. Future work on sediment trap records in the Australian sector will help to clarify the morphologies of *C. leptoporus* in the SAZ. The abundance of *C. leptoporus* at 2000 m was greater than twice that at 500 m during the spring/summer period (Table 3), again possibly the result of some lateral transport of coccoliths.

Helicosphaera carteri exhibited patchy abundances throughout the year, peaking in both spring and autumn/winter (Fig. 7), which likely resulted in it appearing distinct from both groups in the CCA (Fig. 4b). The placement of *H. carteri* closer to the second coccolithophore grouping could reflect its preference for cooler waters, like the majority of the second grouping species.

4.6. Ecology and seasonal succession of diatoms and coccolithophores

This study found evidence largely consistent with the previously diatom succession schemes. All three stages of diatom succession were visible in the 47°S sediment trap assemblages, and corresponded to the stages/groups outlined by previous workers on diatom succession. We presumed that the second stage in diatom succession (i.e. Transitional assemblage group; Fig. 9) was likely to be of shorter duration at depth than in live assemblages. This is believed to be because the signal of early-blooming taxa is small within traps due to dissolution, thus assemblages are soon dominated by Preservation species, which represent the greater fraction of diatoms captured in sediment traps. Of the Transition group, only the presence of *Chaetoceros* resting spores was an undeniable indicator. The Preservation group on the other hand was unmistakeable in sediment traps, being more likely to survive export intact than the other two groups. Selective preservation of heavily silicified diatom species is most likely the main factor determining the strongest evidence for stage 3 diatom succession in the sediment traps (Fig. 9). The links between photic zone production and sediment preservation are complex and unclear, with implications for studies aiming to reconstruct past oceanic conditions using seafloor sediment. Thus, further investigations in both surface layer and sediment traps as well as in other sectors of the circumpolar SAZ are required to better understand the diatom seasonal succession and links between production and export in this region of the world's ocean.

Moreover, the data presented here represents the first seasonal record of coccolithophore species succession in the SAZ. Coccolithophore assemblage composition, registered by the sediment traps, were consistent with previously reported live coccolithophore assemblages in the surface waters of the region. Coccolithophore assemblages were dominated by the ubiquitous species *E. huxleyi*

which represented 59% of the annual assemblage. Two ecological groupings were observed relating to the seasonal succession of coccolithophores captured in traps. The first grouping contained three taxa (*Coccolithus pelagicus, Syracosphaera* spp., and *Gephyrocapsa muellerae*) with seasonality associated with PAR. These species tended to peak within the spring/summer period, and were absent or low in autumn and winter. The second ecological grouping contained taxa either displaying greater abundances outside of the spring/summer period (e.g. *C. leptoporus*), or that were present persistently year-round (such as *E. huxleyi*). The appearance of coccolithophore succession from these sediment trap records was complex, and it is speculated that oceanographic influences, such as warm water intrusion from the north, influenced assemblages captured by the sediment traps. A seasonal evolution scheme of coccolithophore communities, like that of diatoms, remains to be constructed. Further sediment trap studies of seasonal coccolithophore assemblages will allow for a deeper understanding of coccolithophore ecology. Live assemblage sampling in the SAZ, and analyses of coccolithophore assemblages within, will be necessary to begin to identify a generalised successional scheme for this group.

5. Conclusions

This study reports on the biochemical, siliceous and calcareous phytoplankton fluxes registered by a time-series sediment trap deployed during a year in the Australian sector of the SAZ at 500 m and 2000 m depths. The BSi: PIC reflects the high abundance of coccolithophores and other calcareous microplankton in comparison with diatoms (three orders of magnitude lower). The specific contribution of the two phytoplankton groups to POC export could not be quantified, however, it is suggested that coccoliths provide a major source of ballast for settling particles in this sector of the SAZ. Total mass fluxes were seasonal, with the overwhelming majority of material captured between spring and early summer. The maximum particle flux was registered at the same time at both depths, despite a 1500 m vertical disparity between the traps, leading to the inference that particle settling speed was high, at ~100 m d^{-1}.

Diatom assemblages in this study displayed some expected successional trends in keeping with ecological succession theory, with some differences thought to have resulted from the transformation of particles anticipated to have occurred at depth and with particle export. Diatom assemblages were roughly categorised into three ecological groupings: the "PAR group" of fast-proliferating, early blooming species, the "Transition group", and the "Preservation group" of heavily silicified large diatoms. A scheme is presented illustrating the effects of transport through the water column on the appearance of diatom succession from sediment trap records in the SAZ. Further comparison of diatom successional patterns between live and sediment assemblages is warranted to better understand the transformational processes at play in this region. Palaeoreconstructions using preserved diatoms, and particularly those that use diatoms as seasonal signals, rely upon accurately linking surface processes to the sediment. Future clarification of how live diatom assemblage seasonality is reflected in the sediment or in sediment traps will lend greater accuracy to palaeoreconstructive work.

Coccolith assemblages also displayed some successional trends, with two ecological groupings of taxa identified within sediment traps. The precise interaction between these ecological groupings and environmental variables is yet to be determined, and will require further sediment trap analysis. Work on differentiating the morphological variations among coccoliths captured by sediment traps in the Australian sector will be conducted in future studies.

A deeper understanding of the biological and physical processes that control the carbon export in the SAZ is of critical importance to determine of the role of the Southern Ocean in the global cycling of nutrients and climate. The results of the present and previous studies

on the 47ºS site show that the carbon export in the Australian sector of the SAZ is similar to those reported in other zonal systems further south (PFZ and AZ). Coccolithophore-related carbon export has been found to be significant in the SAZ, however, the specific contribution of different species to export, and the expression of coccolithophore seasonality in sediment traps, will be the focus of future trapping studies.

Acknowledgements

Appendix A. Supplementary material

Supplementary data associated with this article can be found in the online version at doi:10.1016/j.dsr.2017.01.001.

References

Alvain, S., Moulin, C., Dandonneau, Y., Loisel, H., 2008. Seasonal distribution and succession of dominant phytoplankton groups in the global ocean: a satellite view. Glob. Biogeochem. Cycles 22.

Anderson, R.F., Smith, W.O., Jr, 2001. The US Southern Ocean joint Global Ocean flux study: volume two. Deep-Sea Res. Part II: Top. Stud. Oceanogr. 48, 3883–3889. http://dx.doi.org/10.1016/S0967-0645(01)00072-8.

Andruleit, H., Stäger, S., Rogalla, U., Čepek, P., 2003. Living coccolithophores in the northern Arabian Sea: ecological tolerances and environmental control. Mar. Micropaleontol. 49, 157–181.

Armand, L.K., Crosta, X., Romero, O., Pichon, J.-J., 2005. The biogeography of major diatom taxa in Southern Ocean sediments: 1. Sea ice related species. Palaeogeography, Palaeoclimatology. Palaeoecology 223, 93–126.

Armand, L.K., Leventer, A., 2010. Palaeo sea ice distribution and reconstruction derived from the geological records. Sea ice, 469–530.

Assmy, P., Smetacek, V., Montresor, M., Klaas, C., Henjes, J., Strass, V.H., Arrieta, J.M., Bathmann, U., Berg, G.M., Breitbarth, E., 2013. Thick-shelled, grazer-protected diatoms decouple ocean carbon and silicon cycles in the iron-limited Antarctic circumpolar current. Proc. Natl. Acad. Sci. 110, 20633–20638.

Balch, W.M., 2004. Re-evaluation of the physiological ecology of coccolithophores. In: Thierstein, H.R., Young, J.R. (Eds.), Coccolithophores: from molecular processes to global impact. Springer Science & Business Media, 156–190.

Balch, W.M., Drapeau, D.T., Bowler, B.C., Lyczskowski, E., Booth, E.S., Alley, D., 2011. The contribution of coccolithophores to the optical and inorganic carbon budgets during the Southern Ocean gas exchange experiment: new evidence in support of the "Great calcite Belt" hypothesis. J. Geophys. Res.: Oceans 1978–2012, 116. http://dx.doi.org/10.1029/2011JC006941.

Balch, W.M., Bates, N.R., Lam, P.J., Twining, B.S., Rosengard, S.Z., Bowler, B.C., Drapeau, D.T., Garley, R., Lubelczyk, L.C., Mitchell, C., Rauschenberg, S., 2016. Factors regulating the Great Calcite Belt in the Southern Ocean and its biogeochemical significance. Glob. Biogeochem. Cycles 30, 1124–1144. http://dx.doi.org/10.1002/2016GB005414.

Baker, E.T., Milburn, H.B., Tennant, D.A., 1988. Field assessment of sediment trap efficiency under varying flow conditions. J. Mar. Res. 46, 573–592.

Blain, S., Tréguer, P., Belviso, S., Bucciarelli, E., Denis, M., Desabre, S., Fiala, M., Jézéquel, V.M., Le Fèvre, J., Mayzaud, P., 2001. A biogeochemical study of the island mass effect in the context of the iron hypothesis: Kerguelen Islands, Southern Ocean. Deep-Sea Res. Part I:Oceanogr. Res.Pap. 48, 163–187.

Boeckel, B., Baumann, K.-H., Henrich, H., Kinkel, H., 2006. Coccolith distribution patterns in South Atlantic and Southern Ocean surface sediments in relation to environmental gradients. Deep-Sea Res. Part I: Oceanogr. Res. Pap. 53, 1073–1099.

Bowie, A.R., Brian Griffiths, F., Dehairs, F., Trull, T.W., 2011. Oceanography of the subantarctic and Polar Frontal Zones south of Australia during summer: Setting for the SAZ-Sense study. Deep-Sea Res. Part II: Top. Stud. Oceanogr. 58, 2059–2070. http://dx.doi.org/10.1016/j.dsr2.2011.05.033.

Boyd, P.W., Watson, A.J., Law, C.S., Abraham, E.R., Trull, T., Murdoch, R., Bakker, D.C.E., Bowie, A.R., Buesseler, K.O., Chang, H., Charette, M., Croot, P., Downing, K., Frew, R., Gall, M., Hadfield, M., Hall, J., Harvey, M., Jameson, G., LaRoche, J., Liddicoat, M., Ling, R., Maldonado, M.T., McKay, R.M., Nodder, S., Pickmere, S., Pridmore, R., Rintoul, S., Safi, K., Sutton, P., Strzepek, R., Tanneberger, K., Turner, S., Waite, A., Zeldis, J., 2000. A mesoscale phytoplankton bloom in the polar Southern Ocean stimulated by iron fertilization. Nature 407, 695–702.

Boyd, P.W., 2013. Diatom traits regulate Southern Ocean silica leakage. Proc. Natl. Acad. Sci. 110, 20358–20359.

Bray, S., Trull, T., Manganini, S., 2000. SAZ project moored sediment traps: results of the 1997–1998 deployments. Antarctic CRC.

Broerse, A.T., Ziveri, P., van Hinte, J.E., Honjo, S., 2000. Coccolithophore export production, species composition, and coccolith-CaCO 3 fluxes in the NE Atlantic (34°N21'W and 48°N21'W). Deep-Sea Res. Part II: Top. Stud. Oceanogr. 47, 1877–1905.

Bucciarelli, E., Blain, S., Tréguer, P., 2001. ron and manganese in the wake of the Kerguelen Islands (Southern Ocean). Mar. Chem. 73, 21–36.

Crosta, X., Romero, O., Armand, L.K., Pichon, J.-J., 2005. The biogeography of major diatom taxa in Southern Ocean sediments: 2. open ocean related species. Palaeogeogr., Palaeoclimatol., Palaeoecol. 223, 66–92.

Cubillos, J., Wright, S., Nash, G., De Salas, M., Griffiths, B., Tilbrook, B., Poisson, A., Hallegraeff, G., 2007. Calcification morphotypes of the coccolithophorid *Emiliania huxleyi* in the Southern Ocean: changes in 2001 to 2006 compared to historical data. Mar. Ecol. Prog. Ser. 348, 47–54.

Cubillos, J.C., Henderiks, J., Beaufort, L., Howard, W.R., Hallegraeff, G.M., 2012. Reconstructing calcification in ancient coccolithophores: individual coccolith weight and morphology of *Coccolithus pelagicus* (sensu lato). Mar. Micropaleontol. 92–93, 29–39. http://dx.doi.org/10.1016/j.marmicro.2012.04.005.

De La Rocha, C.L., Passow, U., 2007. Factors influencing the sinking of POC and the efficiency of the biological carbon pump. Deep-Sea Res. Part II: Top. Stud. Oceanogr. 54, 639–658.

De Salas, M.F., Eriksen, R., Davidson, A.T., Wright, S.W., 2011. Protistan communities in the Australian sector of the Sub-Antarctic Zone during SAZ-Sense. Deep-Sea Res. Part II: Top. Stud. Oceanogr. 58, 2135–2149. http://dx.doi.org/10.1016/j.dsr2.2011.05.032.

Dimiza, M.D., Triantaphyllou, M.V., Dermitzakis, M.D., 2008. Seasonality and ecology of living coccolithophores in eastern Mediterranean coastal environment (Andros Island, middle Aegean Sea). Micropaleontology 54, 159–175. http://dx.doi.org/10.2307/30130910.

Ebersbach, F., Trull, T.W., Davies, D.M., Bray, S.G., 2011. Controls on mesopelagic particle fluxes in the Sub-Antarctic and Polar Frontal Zones in the Southern Ocean south of Australia in summer—Perspectives from free-drifting sediment traps. Deep-Sea Res. Part II: Top. Stud. Oceanogr. 58, 2260–2276.

Fatela, F., Taborda, R., 2002. Confidence limits of species proportions in microfossil assemblages. Mar. Micropaleontol. 45, 169–174.

Findlay, C.S., 1998. Living and fossil calcareous nannoplankton from the Australian sector of the Southern Ocean: implications for paleoceanography (PhD dissertation). University of Tasmania.

Findlay, C.S., Giraudeau, J., 2000. Extant calcareous nannoplankton in the Australian Sector of the Southern Ocean (austral summers 1994 and 1995). Mar. Micropaleontol. 40, 417–439. http://dx.doi.org/10.1016/S0377-8398(00)00046-3.

Fischer, G., Gersonde, R., Wefer, G., 2002. Organic carbon, biogenic silica and diatom fluxes in the marginal winter sea-ice zone and in the Polar Front Region: interannual variations and differences in composition. Deep.-Sea Res. Part II:Top. Stud.Oceanogr. 49, 1721–1745.

Flores, J.-A., Gersonde, R., Sierro, F., Niebler, H.-S., 2000. Southern Ocean Pleistocene calcareous nannofossil events: calibration with isotope and geomagnetic stratigraphies. Mar. Micropaleontol. 40, 377–402.

Flores, J., Sierro, F., 1997. Revised technique for calculation of calcareous nannofossil accumulation rates. Micropaleontology, 321–324.

Fripiat, F., Leblanc, K., Elskens, M., Cavagna, A.-J., Armand, L., André, L., Dehairs, F., Cardinal, D., 2011. Efficient silicon recycling in summer in both the Polar Frontal and Subantarctic Zones of the Southern Ocean. Mar. Ecol. Prog. Ser. 435, 47–61.

Goddard Earth Sciences Data and Information Services Centre (2012, last updated 2013) ⟨http://disc.sci.gsfc.nasa.gov/giovanni#maincontent⟩, accessed 14/07/2014

Gravalosa, J.M., Flores, J.-A., Sierro, F.J., Gersonde, R., 2008. Sea surface distribution of coccolithophores in the eastern Pacific sector of the Southern Ocean (Bellingshausen and Amundsen Seas) during the late austral summer of 2001. Mar. Micropaleontol. 69, 16–25.

Guillard, R.R.L., Kilham, P., 1977. The ecology of marine planktonic diatoms. In: Werner, D. (Ed.), The Biology of Diatoms. Blackwell Oxford, 372–469.

Hammer, Ø., Harper, D.A.T., Ryan, P.D., 2001. PAST: Paleontological statistics software package for education and data analysis. Palaeontol. Electron. 4, 9.

Hasle, G., Syvertsen, E., 1997. Identifying Marine Phytoplankton. Academic Press, San Diego, CA.

Herraiz-Borreguero, L., Rintoul, S.R., 2011. Regional circulation and its impact on upper ocean variability south of Tasmania. Deep-Sea Res. Part II: Top. Stud. Oceanogr. 58, 2071–2081. http://dx.doi.org/10.1016/j.dsr2.2011.05.022.

Honjo, S., Francois, R., Manganini, S., Dymond, J., Collier, R., 2000. Particle fluxes to the interior of the Southern Ocean in the Western Pacific sector along 170°W. Deep-Sea Res. Part II: Top. Stud. Oceanogr. 47, 3521–3548. http://dx.doi.org/10.1016/S0967-0645(00)00077-1.

Honjo, S., Manganini, S.J., Krishfield, R.A., Francois, R., 2008. Particulate organic carbon fluxes to the ocean interior and factors controlling the biological pump: a synthesis of global sediment trap programs since 1983. Prog. Oceanogr. 76, 217–285.

Howard, W.R., Roberts, D., Moy, A.D., Lindsay, M.C.M., Hopcroft, R.R., Trull, T.W., Bray, S.G., 2011. Distribution, abundance and seasonal flux of pteropods in the Sub-Antarctic Zone. Deep-Sea Res. Part II: Top. Stud. Oceanogr. 58, 2293–2300. http://dx.doi.org/10.1016/j.dsr2.2011.05.031.

Hutchins, D.A., Sedwick, P.N., DiTullio, G.R., Boyd, P.W., Quéguiner, B., Griffiths, F.B., Crossley, C., 2001. Control of phytoplankton growth by iron and silicic acid availability in the subantarctic Southern Ocean: experimental results from the SAZ Project. J. Geophys. Res.: Oceans 106, 31559–31572. http://dx.doi.org/10.1029/2000JC000333.

Iversen, M.H., Nowald, N., Ploug, H., Jackson, G.A., Fischer, G., 2010. High resolution profiles of vertical particulate organic matter export off Cape blanc, Mauritania: degradation processes and ballasting effects. Deep-Sea Res. Part I: Oceanogr. Res. Pap. 57, 771–784.

Iversen, M., Ploug, H., 2010. Ballast minerals and the sinking carbon flux in the ocean: carbon-specific respiration rates and sinking velocity of marine snow aggregates. Biogeosciences 7, 2613–2624.

King, A.L., Howard, W.R., 2003. Planktonic foraminiferal flux seasonality in Subantarctic sediment traps: a test for paleoclimate reconstructions. Paleoceanography 18.

King, A.L., Howard, W.R., 2005. δ18O seasonality of planktonic foraminifera from Southern Ocean sediment traps: latitudinal gradients and implications for paleoclimate reconstructions. Mar. Micropaleontol. 56, 1–24. http://dx.doi.org/10.1016/j.marmicro.2005.02.008.

Klaas, C., Archer, D.E., 2002. Association of sinking organic matter with various types of mineral ballast in the deep-sea: implications for the rain ratio. Glob. Biogeochem. Cycles 16, 63–61-63-14.

Kopczyńska, E.E., Dehairs, F., Elskens, M., Wright, S., 2001. Phytoplankton and microzooplankton variability between the Subtropical and Polar Fronts south of Australia: thriving under regenerative and new production in late summer. J. Geophys. Res.: Oceans (1978–2012) 106, 31597–31609.

Kopczyńska, E.E., Savoye, N., Dehairs, F., Cardinal, D., Elskens, M., 2007. spring phytoplankton assemblages in the Southern Ocean between Australia and Antarctica. Polar Biol. 31, 77–88.

Lampitt, R., Antia, A., 1997. Particle flux in deep seas: regional characteristics and temporal variability. Deep-Sea Res. Part I: Oceanogr.Res. Pap. 44, 1377–1403.

Leblanc, K., Hare, C.E., Boyd, P.W., Bruland, K.W., Sohst, B., Pickmere, S., Lohan, M.C., Buck, K., Ellwood, M., Hutchins, D.A., 2005. Fe and Zn effects on the Si cycle and diatom community structure in two contrasting high and low-silicate HNLC areas. Deep-Sea Res. Part I: Oceanogr. Res. Pap. 52, 1842–1864. http://dx.doi.org/10.1016/j.dsr.2005.06.005.

Leventer, A., 1991. Sediment trap diatom assemblages from the northern Antarctic Peninsula region. Deep-Sea Res. Part A. Oceanogr. Res. Pap. 38, 1127–1143. http://dx.doi.org/10.1016/0198-0149(91)90099-2.

Lourey, M.J., Trull, T.W., 2001. Seasonal nutrient depletion and carbon export in the Subantarctic and Polar Frontal Zones of the Southern Ocean south of Australia. J. Geophys. Res.: Oceans 106, 31463–31487.

Malinverno, E., Triantaphyllou, M.V., Dimiza, M.D., 2015. Coccolithophore assemblage distribution along a temperate to polar gradient in the West Pacific sector of the Southern Ocean (January 2005). Micropaleontology 61, 489–506.

Malinverno, E., Maffioli, P., Gariboldi, K., 2016. Latitudinal distribution of extant fossilizable phytoplankton in the Southern Ocean: planktonic provinces, hydrographic fronts and palaeoecological perspectives. Mar. Micropaleontol. 123, 41–58.

Margalef, R., 1978. Life-forms of phytoplankton as survival alternatives in an unstable environment. Oceanol. Acta 1, 493–509.

Metzl, N., Tilbrook, B., Poisson, A., 1999. The annual fCO₂ cycle and the air–sea CO₂ flux in the sub-Antarctic Ocean. Tellus B 51, 849–861.

Nishida, S., 1986. Nannoplankton flora in the Southern Ocean, with special reference to siliceous varieties. Mem. Natl. Inst. Polar Res. 40, 56–68.

Nodder, S.D., Northcote, L.C., 2001. Episodic particulate fluxes at southern temperate mid-latitudes (42–45 S) in the Subtropical Front region, east of New Zealand. Deep-Sea Res. Part I: Oceanogr. Res. Pap. 48, 833–864.

Nodder, S.D., Chiswell, S.M., Northcote, L.C., 2016. Annual cycles of deep-ocean biogeochemical export fluxes in subtropical and subantarctic waters, southwest Pacific ocean. J. Geophys. Res.: Oceans 121, 2405–2424. http://dx.doi.org/10.1002/2015JC011243.

Olguín, H.F., Alder, V.A., 2011. Species composition and biogeography of diatoms in antarctic and subantarctic (Argentine shelf) waters (37–76 S). Deep Sea Res. Part II: Top. Stud. Oceanogr. 58, 139–152.

Orsi, A.H., Whitworth, T., Nowlin, W.D., 1995. On the meridional extent and fronts of the Antarctic circumpolar Current. Deep-Sea Res. Part I: Oceanogr. Res. Pap. 42, 641–673.

Patil, S.M., Mohan, R., Shetye, S., Gazi, S., Jafar, S., 2014. Morphological variability of *Emiliania huxleyi* in the Indian sector of the Southern Ocean during the austral summer of 2010. Mar. Micropaleontol. 107, 44–58.

Pollard, R., Lucas, M., Read, J., 2002. Physical controls on biogeochemical zonation in the Southern Ocean. Deep-Sea Res. Part II: Top. Stud. Oceanogr. 49, 3289–3305.

Quéguiner, B., 2001. Biogenic silica production in the Australian sector of the Subantarctic zone of the Southern Ocean. J. Geophys. Res. 106, 31,627–631,636.

Quéguiner, B., 2013. Iron fertilization and the structure of planktonic communities in high nutrient regions of the Southern Ocean. Deep-Sea Res. Part II: Top. Stud. Oceanogr. 90, 43–54. http://dx.doi.org/10.1016/j.dsr2.2012.07.024.

Ragueneau, O., Tréguer, P., Leynaert, A., Anderson, R.F., Brzezinski, M.A., DeMaster, D.J., Dugdale, R.C., Dymond, J., Fischer, G., François, R., Heinze, C., Maier-Reimer, E., Martin-Jézéquel, V., Nelson, D.M., Quéguiner, B., 2000. A review of the Si cycle in the modern ocean: recent progress and missing gaps in the application of biogenic opal as a paleoproductivity proxy. Glob. Planet. Change 26, 317–365. http://dx.doi.org/10.1016/S0921-8181(00)00052-7.

Rembauville, M., Meilland, J., Ziveri, P., Schiebel, R., Blain, S., Salter, I., 2016. Planktic foraminifer and coccolith contribution to carbonate export fluxes over the central Kerguelen Plateau. Deep-Sea Res. Part I: Oceanogr. Res. Pap. 111, 91–101. http://dx.doi.org/10.1016/j.dsr.2016.02.017.

Rigual-Hernández, A.S., Bárcena, M.A., Jordan, R.W., Sierro, F.J., Flores, J.A., Meier, K.S., Beaufort, L., Heussner, S., 2013. Diatom fluxes in the NW Mediterranean: evidence from a 12-year sediment trap record and surficial sediments. J. Plankton Res. 35, 1109–1125.

Rigual-Hernández, A.S., Trull, T.W., Bray, S.G., Closset, I., Armand, L.K., 2015a. Seasonal dynamics in diatom and particulate export fluxes to the deep-sea in the Australian sector of the southern Antarctic Zone. J. Mar. Syst. 142, 62–74. http://dx.doi.org/10.1016/j.jmarsys.2014.10.002.

Rigual-Hernández, A., Trull, T., Bray, S., Cortina, A., Armand, L., 2015b. Latitudinal and temporal distributions of diatom populations in the pelagic waters of the Subantarctic and Polar Frontal zones of the Southern Ocean and their role in the biological pump. Biogeosciences 12, 5309–5337.

Rigual-Hernández, A.S., Trull, T.W., Bray, S.G., Armand, L.K., 2016b. The fate of diatom valves in the Subantarctic and polar frontal zones of the Southern Ocean: sediment trap versus surface sediment assemblages. Palaeogeogr., Palaeoclimatol., Palaeoecol. 457, 129–143. http://dx.doi.org/10.1016/j.palaeo.2016.06.004.

Rintoul, S.R., Griffiths, F.B., 2001. A persistent subsurface chlorophyll maximum in the. J. Geophys. Res. 106, 31,543–531,557.

Rintoul, S.R., Trull, T.W., 2001. Seasonal evolution of the mixed layer in the Subantarctic zone south of Australia. J. Geophys. Res.: Oceans 106, 31447–31462.

Roberts, D., Howard, W.R., Moy, A.D., Roberts, J.L., Trull, T.W., Bray, S.G., Hopcroft, R.R., 2011. Interannual pteropod variability in sediment traps deployed above and below the aragonite saturation horizon in the Sub-Antarctic Southern Ocean. Polar Biol. 34, 1739–1750.

Romero, O., Armand, L., Crosta, X., Pichon, J.-J., 2005a. The biogeography of major diatom taxa in Southern Ocean surface sediments: 3. tropical/subtropical species. Palaeogeogr., Palaeoclimatol., Palaeoecol. 223, 49–65.

Romero, O., Lange, C., Fischer, G., Treppke, U., Wefer, G., 1999. Variability in export production documented by downward fluxes and species composition of marine planktic diatoms: observations from the tropical and equatorial Atlantic. In: Use of Proxies in Paleoceanography. Springer, 365–392.

Romero, O., Fischer, G., Lange, C., Wefer, G., 2000. Siliceous phytoplankton of the western equatorial Atlantic: sediment traps and surface sediments. Deep-Sea Res. Part II: Top. Stud. Oceanogr. 47, 1939–1959.

Romero, O., Armand, L., Crosta, X., Pichon, J.-J., 2005b. The biogeography of major diatom taxa in Southern Ocean surface sediments: 3. tropical/subtropical species. Palaeogeogr., Palaeoclimatol., Palaeoecol. 223, 49–65.

Romero O., Armand L., 2010. Marine diatoms as indicators of modern changes in oceanographic conditions. In: Smol, J., Stoermer, E., (Eds.). The diatoms: applications for the environmental and earth sciences, pp. 373–400.

Saavedra-Pellitero, M., Baumann, K.-H., Flores, J.-A., Gersonde, R., 2014. Biogeographic distribution of living coccolithophores in the Pacific sector of the Southern Ocean. Mar. Micropaleontol. 109, 1–20.

Sancetta, C., Calvert, S.E., 1988. The annual cycle of sedimentation in Saanich Inlet, British Columbia: implications for the interpretation of diatom fossil assemblages. Deep-Sea Res. Part A. Oceanogr.Res. Pap. 35, 71–90.

Salter, I., Schiebel, R., Ziveri, P., Movellan, A., Lampitt, R., Wolff, G.A., 2014. Carbonate counter pump stimulated by natural iron fertilization in the Polar Frontal Zone. Nat. Geosci. 7, 885–889.

Schiebel, R., 2002. Planktic foraminiferal sedimentation and the marine calcite budget. Glob. Biogeochem. Cycles 16.

Schlitzer R., 2016. Ocean Data View Software, ⟨http://odv.awi.de⟩.

Scholten, J.C., Fietzke, J., Vogler, S., Rutgers van der Loeff, M.M., Mangini, A., Koeve, W., Waniek, J., Stoffers, P., Antia, A., Kuss, J., 2001. Trapping efficiencies of sediment traps from the deep eastern North Atlantic: the 230Th calibration. Deep-Sea Res. Part II: Top. Stud. Oceanogr. 48, 2383–2408. http://dx.doi.org/10.1016/S0967-0645(00)00176-4.

Sedwick, P.N., DiTullio, G.R., Hutchins, D.A., Boyd, P.W., Griffiths, F.B., Crossley, A.C., Trull, T.W., Quéguiner, B., 1999. Limitation of algal growth by iron deficiency in the Australian Subantarctic Region. Geophys. Res. Lett. 26, 2865–2868.

Sedwick, P., Bowie, A., Trull, T., 2008. Dissolved iron in the Australian sector of the Southern Ocean (CLIVAR SR3 section): Meridional and seasonal trends. Deep-Sea Res. Part I: Oceanogr. Res. Pap. 55, 911–925.

Shadwick, E., Trull, T., Tilbrook, B., Sutton, A., Schulz, E., Sabine, C., 2015. Seasonality of biological and physical controls on surface ocean CO₂ from hourly observations at the Southern Ocean time series site south of Australia. Glob. Biogeochem. Cycles 29, 223–238.

Shannon, C.E., Weaver, W., 1949. The mathematical theory of communication (Dissertation). University of Illinois.

Smetacek, V., Assmy, P., Henjes, J., 2004. The role of grazing in structuring Southern Ocean pelagic ecosystems and biogeochemical cycles. Antarct. Sci. 16, 541–558.

Smith, W.O., Anderson, R.F., Moore, J.K., Codispoti, L.A., Morrison, J.M., 2000. The US southern ocean joint global ocean flux study: an introduction to AESOPS. Deep-Sea Res. Part II: Top. Stud. Oceanogr. 47, 3073–3093.

Sokolov, S., Rintoul, S.R., 2002. Structure of Southern Ocean fronts at 140 E. J. Mar. Syst. 37, 151–184.

Steinmetz, J.C., 1994. Sedimentation of coccolithophores. Coccolithophores, 179–198.

Ternois, Y., Sicre, M.-A., Boireau, A., Beaufort, L., Miquel, J.-C., Jeandel, C., 1998. Hydrocarbons, sterols and alkenones in sinking particles in the Indian Ocean sector of the Southern Ocean. Org. Geochem. 28, 489–501.

Thunell, R., Pride, C., Ziveri, P., Muller-Karger, F., Sancetta, C., Murray, D., 1996.

Plankton response to physical forcing in the Gulf of California. J. Plankton Res. 18, 2017–2026.

Treppke, U.F., Lange, C.B., Wefer, G., 1996. Vertical fluxes of diatoms and silicoflagellates in the eastern equatorial Atlantic, and their contribution to the sedimentary record. Mar. Micropaleontol. 28, 73–96.

Trull, T., Bray, S., Manganini, S., Honjo, S., Francois, R., 2001a. Moored sediment trap measurements of carbon export in the Subantarctic and Polar Frontal zones of the Southern Ocean, south of Australia. J. Geophys. Res.: Oceans (1978–2012) 106, 31489–31509.

Trull, T., Rintoul, S.R., Hadfield, M., Abraham, E.R., 2001b. Circulation and seasonal evolution of polar waters south of Australia: implications for iron fertilization of the Southern Ocean. Deep-Sea Res. Part II: Top. Stud. Oceanogr. 48, 2439–2466.

Trull, T., Sedwick, P., Griffiths, F., Rintoul, S., 2001c. Introduction to special section: SAZ Project. J. Geophys. Res.: Oceans (1978–2012) 106, 31425–31429.

Tyrrell, T., Merico, A., 2004. Emiliania huxleyi: bloom observations and the conditions that induce them. In: Coccolithophores. Springer, pp. 75–97.

Wefer, G., Fischer, G., 1991. Annual primary production and export flux in the Southern Ocean from sediment trap data. Mar. Chem. 35, 597–613.

Westwood, K.J., Griffiths, F.B., Webb, J.P., Wright, S.W., 2011. Primary production in the Sub-Antarctic and Polar Frontal zones south of Tasmania, Australia; SAZ-Sense survey, 2007. Deep Sea Res. Part II: Top. Stud. Oceanogr. 58, 2162–2178.

Winter, A., Henderiks, J., Beaufort, L., Rickaby, R.E., Brown, C.W., 2014. Poleward expansion of the coccolithophore *Emiliania huxleyi*. J. Plankton Res. 36, 316–325.

Young, J., Geisen, M., Cros, L., Kleijne, A., Sprengel, C., Probert, I., Østergaard, J., 2003. A guide to extant coccolithophore taxonomy. J. Nannoplankton Res. Spec. 1, 1–124.

Young J., Bown P., Lees J., 2014. Nannotax3 website. International Nannoplankton Association. ⟨http://ina.tmsoc.org/Nannotax3⟩.(accessed 21.04.14)

Yu, E.F., Francois, R., Bacon, M.P., Honjo, S., Fleer, A.P., Manganini, S.J., Rutgers van der Loeff, M.M., Ittekot, V., 2001. Trapping efficiency of bottom-tethered sediment traps estimated from the intercepted fluxes of 230Th and 231Pa. Deep-Sea Res. Part I: Oceanogr. Res. Pap. 48, 865–889. http://dx.doi.org/10.1016/S0967-0637(00) 00067-4.

Zielinski, U., Gersonde, R., 1997. Diatom distribution in Southern Ocean surface sediments (Atlantic sector): implications for paleoenvironmental reconstructions. Palaeogeogr. Palaeocl. 129, 213–250. http://dx.doi.org/10.1016/S003-0182(96) 00130-73.

Ziveri, P., Rutten, A., De Lange, G., Thomson, J., Corselli, C., 2000. Present-day coccolith fluxes recorded in central eastern Mediterranean sediment traps and surface sediments. Palaeogeogr., Palaeoclimatol., Palaeoecol. 158, 175–195.